

## Article

# Lipid Fractionation and Physicochemical Characterization of *Carapa guianensis* Seed Oil from Guyana

Stacy O. James, Laziz Bouzidi, R. J. Neil Emery  and Suresh S. Narine \*

Trent Centre for Biomaterials Research, Departments of Physics & Astronomy and Chemistry, Trent University, 1600 West Bank Drive, Peterborough, ON K9J 7B8, Canada; stacyjames@trentu.ca (S.O.J.); lazizbouzidi@trentu.ca (L.B.); nemery@trentu.ca (R.J.N.E.)

\* Correspondence: sureshnarine@trentu.ca

**Abstract:** The seed oil of *Carapa guianensis*, known as crabwood oil (CWO), is distinguished for its medicinal and cosmetics applications, attributed to its bioactive components and lipid profile. CWO and its dry and solvent fractionation were studied, with a focus on physicochemical functionality and the partitioning of known bioactive compounds, such as limonoids and sterols. Important bioactive components, including limonoids and sterols, were partitioned depending on the fractionation method; in particular, there is a direct dependence on solvent polarity. There was a very strong solid fraction yield–solvent polarity with a high linear slope of  $-121.3\%$ . The partitioning of the lipids is significant enough to drive measurable and predictable changes in the physical properties. Palmitic (P: C16:0) and oleic (O: C18:1) fatty acids account for about 60% of the total fatty acid composition of the TAGs of CWO and its fractions. The most abundant limonoid is methyl angolensate (from 28 to 39%), followed by Trichilin A (from 13% to 22%). Gedunin and Andirobin were more abundant in the liquid fractions, whereas Carapanolides (less than 1.3%) were more present in the olein fractions. The crystallization and melting temperatures of the solid fractions were up to  $26\text{ }^{\circ}\text{C}$ , compared to  $11\text{ }^{\circ}\text{C}$  for CWO, and were particularly strongly correlated to the polarity of the solvents. The SFC profile indicated semi-solid fats, with the solid fractions showing up to 19% at  $18\text{ }^{\circ}\text{C}$ , twice the SFC in CWO. The fractions demonstrated a wide range of distinguishable microstructures. The shapes include well-organized spherulites and needle-like and rod-like crystals with sizes varying from 5 to  $250\text{ }\mu\text{m}$ , suggesting that they are likely to have different flow characteristics and feel to the skin and mouth. There is a potential to make unique compositions with significantly different properties, with antimicrobial and antifungal efficacy due to the bioactive components of CWO through fractionation, using polarity as a predictive tool.

**Keywords:** *Carapa guianensis*; crabwood oil (CWO); dry fractionation; solvent fractionation; chemical profile; lipids; bioactive compounds; physical properties



**Citation:** James, S.O.; Bouzidi, L.; Emery, R.J.N.; Narine, S.S. Lipid Fractionation and Physicochemical Characterization of *Carapa guianensis* Seed Oil from Guyana. *Processes* **2023**, *11*, 2565. <https://doi.org/10.3390/pr11092565>

Academic Editor: Dariusz Dziki

Received: 3 August 2023

Revised: 22 August 2023

Accepted: 25 August 2023

Published: 27 August 2023



**Copyright:** © 2023 by the authors. Licensee MDPI, Basel, Switzerland. This article is an open access article distributed under the terms and conditions of the Creative Commons Attribution (CC BY) license (<https://creativecommons.org/licenses/by/4.0/>).

## 1. Introduction

Guyana covers an area of 215,000 square kilometers, approximately 85% of which is covered by old-growth standing forests. The country's floral diversity includes over 8000 species, of which 6500 are identified [1]. Amid this biodiversity, the *Carapa* Aublet species, commonly referred to as Crabwood and Andiroba, from the *Meliaceae* family of flowering plants, receives special attention because of its potentially high economic value [2,3]. Crabwood trees are native to tropical and subtropical regions and thrive in the rich soils found in swamps, alluvial flats, marshes and uplands of South and Central America, the Caribbean and tropical Africa [4–6]. The following three species of Crabwood are found in Guyana: *Carapa guianensis*, the most predominant, *Carapa akuri* and *Carapa surinamensis* [7].

The extracts from the crabwood tree, especially the oil extracted from its seeds, known as crabwood oil (CWO), have been recognized in traditional medicine for several centuries [4]. The extract from the leaves, bark and seeds is traditionally used

to improve wound healing and treat various conditions, such as fungal infections [8], malaria [9] and fever [10]. CWO has been used as an itch-relieving, insect-repelling [11], anti-inflammatory [12], antimalarial [13] and skin-protecting medicine [14]. CWO is actively investigated in the scientific community, reaching beyond the ethno-medicinal uses to less traditional applications. The pharmaceutical and homeopathic industries sell the oil in capsules advertised to treat various conditions, including diabetes and rheumatism [13]. Some pharmacies in Georgetown, Guyana, process the oil into soap, candles and insecticidal washes [3]. CWO is also used in modern-day formulations, including in shampoos, salves, creams and other emulsified cosmetics [15,16]. Guyana's National Institute of Applied Science and Technology has formulated a medicated face wash from CWO, widely used to treat chronic acne [17].

Chemically, CWO is composed of two main groups, lipids and non-saponifiable phytochemical compounds. The lipid portion of the oil represents 95–98% of the oil's composition [18]. The remaining 2–5% non-saponifiable component includes structurally varied secondary metabolites, mostly highly oxygenated limonoids, but also flavonoids, sterols and phenolic compounds, which are attributed to the oil's biological activities and its bitter taste [19]. The presence and yields of the oil's constituents may be affected by interspecies variations, environmental conditions and extraction methods. However, these variations are not always manifested visibly [20].

The lipid component of CWO is comprised of primarily triacylglycerols (TAGs) and other minor components, including free fatty acids (FFAs), diacylglycerols (DAGs), monoacylglycerols (MAGs) and phospholipids [18,20,21]. The unsaturated fatty acids percentages have been reported to be up to 60% [22]. The reported lipid fraction consists of up to 67% TAG, 10% DAG, 20% MAG and FFA. 1,2-dioleoyl-3-palmitoyl-glycerol (POO) is the most abundant TAG, accounting for approximately 20% of all the TAGs present. Other reported TAGs include 1-palmitoyl-2-palmitoyl-3-oleoyl-glycerol (PPO), 1-palmitoyl-2-stearoyl-3-oleoyl-glycerol (POS) and triolein (OOO). Together, these make up less than half the content of POO in CWO [18].

The medicinal and other technological applications of CWO have been an active area of research [23]. For example, biocatalysis and enzymatic catalysis have been used to transform CWO into materials suitable for biomedical and industrial applications [24,25]. Free fatty acid amides (FFAA) with anticonvulsant properties have been produced using biocatalysts [25]. CWO has been used for the preparation of biodiesel by enzymatic catalysis [24]. Excellent physicochemical properties and activity against *Aedes aegypti* have been reported for nanoparticles made of silk fibroin with esters obtained from the oil of *Carapa guianensis* [26]. The waste products of CWO have also been tested for the production of sustainable new materials, such as adsorbents or microporous activated carbon for CO<sub>2</sub> capture [27,28].

The physical properties of CWO have been well characterized, including quality and identity parameters, such as acid index, peroxide value, iodine value, FFAs, ester index and viscosity [18]. Studies that consider the plant ecology, seed harvest and processing conditions are scarce and dispersed, even though they are potentially important to the oil's chemical composition, bioactivity and physicochemical properties, and hence its efficient and sustainable use [18,29–31].

Like other tropical oils, such as palm oil [32], coconut oil and shea butter [33], which are commonly fractionated to make specialty materials [34], CWO can be fractionated into solid (stearin) and liquid (olein) fractions. The fractionation of CWO is a potential avenue to amplify the uses and bioactivity of the oil, but it has been reported only once for *Carapa grandiflora*, a species of crabwood found in Western Africa [35]. The authors used dry fractionation and with acetone reported yields of 41% for the solid fraction from dry fractionation and 53% for the soluble fraction from acetone. *Carapa guianensis*, which has approximately 30% total saturated fatty acids compared to 40% for *Carapa grandiflora* [18–36], is expected to provide very different stearin and olein fractions. CWO fractionation, as a

means to extend and amplify the use of the oil, is more challenging than the other tropical oils because of its high unsaturation levels.

This communication describes the fractionation of *C. Guianensis* seed oil (CWO) sourced from Guyana using dry and solvent fractionation with the following three different solvents of varying polarity: ethanol, acetone and ethyl acetate. The selection of the three solvents was based on polarity/pKa and selectivity criteria. A targeted fractionation of CWO, which comprises lipids and bioactive compounds, is challenging because of the delicate balance between crystallization and selective extraction using solvents. Ethyl acetate, acetone and ethanol are included in a range of polarities, which would allow to measurably adjust fractionation yield and chemical composition. This approach is also intended to improve our understanding of polarity's impact on the partitioning of the different compounds by fractionation and possibility of using polarity or pKa as a predictability tool.

The hazard risks and toxicity of the solvents are considered. Ethyl acetate, acetone and ethanol are flammable volatile organic compounds. Ethyl acetate vapor/air mixtures are explosive, its inhalation can lead to irritations and impaired coordination [37], cause organ damage, central nervous system depression and can even be lethal in cases of severe exposure [38]. Acetone and ethanol are both safer when compared to ethyl acetate, with ethanol being the less harmful solvent unless consumed in high quantities [39,40].

Sustainability, availability and cost are also to be considered in the case of industrial scale use. In this regard, ethanol would be advantageous for solvent-mediated fractionation processes. Ethanol is manufactured in Guyana, widely available and relatively affordable making it an effective and sustainable solvent choice for solvent-mediated fractionation for the local cosmetic and pharmaceutical industries.

Established phytochemical and physicochemical functionality analysis methods were utilized to compare the composition and physical functionality of the solid (stearin) and liquid (olein) fractions. The chemical compositions of the fractions were determined by ESI-MS and metabolomic analyses, as typically performed for the characterization of similar seed oils [41].

## 2. Materials and Analytical Methods

### 2.1. Materials

Two samples of naturally separated crabwood oil, so-called Native SOLID ( $N_{\text{SOLID}}$ ) and Native LIQUID ( $N_{\text{LIQUID}}$ ), were purchased in August 2021 in Georgetown, Guyana, from A. Leitch (Georgetown, Guyana) for GYD 2000 or ~USD 13/L. They were obtained by letting CWO sit at ambient temperature and then decanting the liquid from the solid. Unseparated CWO was purchased from the same supplier in July 2023. The native and separated CWO samples were produced from seeds collected by hand from the forest floor at Ebini Upper Demerara Berbice, Guyana and extracted there using an artisanal method. In this method, the seeds are cleaned of debris with stream water, boiled in fresh water for about 12 h, then removed from the water and stored in a cool and dry area for 2–3 weeks. The seeds are then shelled and the kernel is directly exposed to sunlight on galvanized roofing sheets and hand-kneaded to collect the oil in bottles. A semi-porous bag is eventually used to press the remaining oil [29,42]. Ethanol, acetone and ethyl acetate (purity >90%), HPLC grade chloroform and methanol (Sigma-Aldrich, Oakville, ON, Canada) were purchased from VWR, Mississauga, ON, Canada.

### 2.2. Crabwood Oil Fractionation

CWO was fractionated using dry fractionation and solvent fractionation with ethanol, acetone and ethyl acetate. Before fractionation, the oil was fully melted using a water bath at 40–45 °C.

#### 2.2.1. Dry Fractionation

Dry fractionation was performed following a method from the literature [43]. It was conducted under stirring using a 2-liter jacketed reactor fitted with an Isotemp™

temperature regulating system (Fisher Scientific, Waltham, MA, USA). The temperature, which was first set at 40 °C under stirring at 50 rpm for 10 min, was reduced by 1 °C/h to room temperature (RT= 18 °C) and then left at RT for 15 h under 50 rpm stirring. The resulting slurry was then cooled at 1 °C/h to 15 °C and kept at 15 °C under 250 rpm stirring for 17 h. The liquid fraction was then filtered using Fisherbrand P8 filter paper under moderate vacuum.

### 2.2.2. Solvent Fractionation

The fractionation with solvents was performed according to an established method [44]. In each solvent fractionation, 4 parts solvent were added to 1 part of the fully melted CWO: 200 g CWO was used for fractionations with ethanol and acetone and 50 g CWO for the fractionation with ethyl acetate. The mixture was stored at 4 °C for 72 h to allow the stearin to solidify while the olein remained liquid. The mixture was stirred at 50 rpm for 24 h before filtration. The soluble and the insoluble components were separated using Fisherbrand P8 filter paper under moderate vacuum. The solvent was removed by rotary evaporation (vacuum = 15 psi, bath temperature = 30–40 °C) and slow rotation (30 rpm). The fractions were weighed, stored in closed glass bottles and kept refrigerated at 4 °C until further analysis.

## 2.3. Methods

### 2.3.1. Electrospray Ionization Mass Spectrometry

Electrospray ionization mass spectrometry (ESI-MS) was performed on a QExactive Orbitrap mass spectrometer (Thermo Scientific, San Jose, CA, USA, resolution of 140,000 full width at half maximum (FWHM); at 200  $m/z$ ). The Orbitrap was calibrated daily using Pierce™ LTQ ESI positive ion calibration solution (Thermo Scientific). The samples (1 ppm  $w/v$ ) were prepared using chloroform: methanol (70:30  $v/v$ ). The data were processed using the Qual Browser tool of the Thermo Xcalibur software version 3.1 (Thermo Scientific).

### 2.3.2. Differential Scanning Calorimetry (DSC)

The thermal transition behavior was determined using a Q200 DSC (TA Instruments, Newcastle, DE, USA) equipped with a refrigerated cooling system. The sample (4–6 mg) in hermetic aluminum pans was equilibrated at 60 °C for 5 min to erase the thermal history, then cooled at 5 °C/min down to –60 °C where it was held isothermally for 5 min, and then heated back to 60 °C at 10 °C/min.

### 2.3.3. Solid Fat Content Measurements

The solid fat content (SFC) was measured on a Bruker Minispec mq 20 (Bruker, Milton, ON, Canada) pulsed NMR spectrometer equipped with a combined high- and low-temperature probe and a BVT3000 temperature controller (Bruker Ltd.). Liquid nitrogen was used for tempering. The fully melted sample was pipetted into the bottom of an NMR tube filling its bottom 1 cm ( $\sim 0.57 \pm 0.05$  mL), stored at RT ( $18 \pm 1$  °C) and at 4 °C both for 8–10 days and measured at these temperatures. The samples were also melted in situ and progressively cooled down in 2 °C- steps and measured at each temperature isothermally until a plateau is reached. Bruker's Minispec V2.58 Rev12 and Minispec plus V1.1 Rev05 software were used to collect the SFC data.

### 2.3.4. Polarized Light Microscopy

A Leica DM2500P (Leica Microsystems, Wetzlar, Germany) fitted with a Linkam LS 350 temperature-controlled stage (Linkam Scientific Instruments, Tadworth, Surrey, UK) was used to image the microstructure of the crabwood oil and its fractions. The sample was heated to 40 °C to obtain a homogenous melt then a small drop was carefully placed between a preheated glass slide and coverslip to obtain a thin and uniform layer. The samples were then left at RT (18 °C) for 7–10 days to allow the fat to crystallize. The samples

were imaged under cross-polarizers and captured using a digital camera (DFC 420C, Leica Microsystems) mounted to the PLM.

#### 2.3.5. X-ray Diffraction

The X-ray diffraction (XRD) measurements were performed on an Empyrean X-ray diffractometer equipped with Cu-K $\alpha$  radiation operated at 45 kV and 40 mA, and a PIXcel<sup>3D</sup> detector (PANalytical B.V., Lelyweg, The Netherlands). The sample was melted at 40 °C, then loaded into preheated glass capillary tubes (Hampton Research, Aliso Viejo, CA, USA), left to crystallize at RT= 18 °C for 7–10 days, then measured at RT. The XRD patterns were recorded between 0.5° and 36° ( $2\theta$ ) in 0.013° steps, with 250 s intervals. The procedure was automated and controlled by PANalytical's Data Collector (V 3.0a) software. The regions of wide-angle X-ray diffraction scattering (WAXD,  $2\theta > 15^\circ$ ) and small-angle X-ray diffraction scattering (SAXD,  $2\theta < 15^\circ$ ), which fingerprint the subcell structures and the molecules layer order along the normal direction, respectively, were analyzed similar to other fatty compounds [45,46].

#### 2.3.6. Thermogravimetric Analysis

The thermogravimetric analysis (TGA) of CWO and its fractions was conducted on a Q500 (TA Instruments, Newcastle, DE, USA). The sample (10–15 mg) was heated from 25 °C to 600 °C at 10 °C/min under a nitrogen flow of 60.0 mL/min. The onset temperature of mass loss was determined at 5%  $w/w$  ( $T_{5\%}^{on}$ ) as is typical in the field [47]. The derivative of the TGA (DTG) was used to assess the mechanisms of mass loss.

#### 2.4. Statistical Analysis

One sample of  $N_{SOLID}$  and  $N_{LIQUID}$ , and CWO were used for the experiments. The fractionations were not performed in replicates. The physical properties were performed, at least in duplicates. Analysis of variance (ANOVA) followed by the Tukey test was conducted to assess group differences and determine the relationship between the variables measured in each experiment. Pearson product-moment correlation analysis, which describes the linear relationship between two quantitative variables, was conducted to determine the strength and positive or negative nature of the correlation. The statistical analysis was performed using the Sigmastat module of Sigmaplot 12.5 software.

### 3. Results and Discussion

The solid and liquid fractions of CWO obtained by dry and solvent fractionation are conventionally referred to as stearins and oleins, respectively. "Soluble Fraction" refers to the component, which dissolved in the solvent and was collected by rotary evaporation, and "Insoluble Fraction" refers to the component that precipitated and was collected by vacuum filtration.

As verified by visual observation and confirmed by DSC (see Section 3.3 below), the soluble component of CWO in ethanol and acetone presented the characteristics of stearin (SOLID) fractions and their insoluble component, the characteristics of olein (LIQUID) fractions, whereas the soluble component in ethyl acetate was an olein and the insoluble component a stearin. Given that the fractionation conditions were similar, this result is primarily attributed to the decrease in affinity for the oil's components as the polarity decreases. The preferential distribution of the lipids according to polarity is confirmed by the MS analysis of these fractions (see Section 3.2.1).

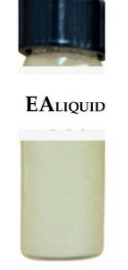
The nomenclature used in this work is shown in Table 1.

**Table 1.** Nomenclature of crabwood oil samples and fractions.

	Name	Abbreviation
As purchased	Native Solid CWO	N <sub>SOLID</sub>
	Native Liquid CWO	N <sub>LIQUID</sub>
	Unseparated Crabwood Oil	CWO
Fractions		
Dry Fractionation	Dry Solid	D <sub>SOLID</sub>
	Dry Liquid	D <sub>LIQUID</sub>
With Ethanol (Et)	Soluble in Et	ET <sub>SOLID</sub>
	Insoluble in Et	ET <sub>LIQUID</sub>
With Acetone (Ac)	Soluble in Ac	AC <sub>SOLID</sub>
	Insoluble in Ac	AC <sub>LIQUID</sub>
With Ethyl Acetate (EA)	Soluble in EA	EA <sub>LIQUID</sub>
	Insoluble in EA	EA <sub>SOLID</sub>

### 3.1. Fractionation Results

Pictures of the fractions in transparent glass bottles taken after 8–10 days at RT (18 °C) are shown in Figure 1. The color of the fractions is noted below each image.

	CWO	N <sub>SOLID</sub>	D <sub>SOLID</sub>	EA <sub>SOLID</sub>	AC <sub>SOLID</sub>	ET <sub>SOLID</sub>
<b>Picture</b>						
<b>Color</b>	Light Amber	Light yellow	White	Ivory	Light yellow	Ivory
<b>Texture</b>	Flows freely	Melts on skin contact	Melts on skin contact	Melts on skin contact	Melts on skin contact	Melts on skin contact
		N <sub>LIQUID</sub>	D <sub>LIQUID</sub>	EA <sub>LIQUID</sub>	AC <sub>LIQUID</sub>	ET <sub>LIQUID</sub>
<b>Picture</b>						
<b>Color</b>		Amber	Amber	Ivory	Off white	Light amber
<b>Texture</b>		sedimented crystals	sedimented crystals	Melts on skin contact	Melts on skin contact	Dispersed and sedimented crystals

**Figure 1.** Physical appearance of CWO and the fractions at room temperature (RT = 18 °C).

### Mass Balance and Yield

The yields obtained from the different fractionations of CWO are presented in Table 2. The oil and fat losses were weighed from the filter paper and the glass vessels. The losses from the filters and vessels represented approximately 40% and 60% of the total loss, respectively.

**Table 2.** Mass balance and yields for crabwood oil dry and solvent (ethyl acetate, acetone and ethanol) fractionation. Relative polarity and pKa values [48] NA: not applicable.

Method	Relative Polarity	pKa	CWO Mass (g)	Mass Loss (g)	Mass Loss (%)	Mass Result (g)			Solid Fraction Yield (%)
						Solid	Liquid	Total	
Dry	NA	NA	258	3.4	1.3	74.8	177.5	252.3	29.3
Ethyl Acetate	0.228	25	50	3.5	7.0	3.1	43.5	46.6	6.2
Acetone	0.355	20	200	5.5	2.7	148.3	46.3	194.6	74.1
Ethanol	0.654	15.9	200	4.7	2.4	80.6	114.7	195.3	40.3

The yields of the soluble fraction increased steadily from the fractionation with ethanol, the most polar, to ethyl acetate, the least polar. The uncertainty about the measurements is less than 5%. Given all the other conditions of the fractionation were similar, this result is primarily attributed to a monotonous variation in the affinity of the solvent for the oil's components as the polarity decreases. The decrease in the yield with increasing polarity is consistent with the decrease in solubility, in polar solvents, of TAGs, which are the main components of CWO [49]. The Pearson analysis indicated a very strong negative linear correlation between the yields of the soluble fractions and relative polarities ( $r = -0.9994$ , Figure 2). The slope of the correlation is high ( $-121.3\%$ /relative unit), and given all other fractionation conditions are the same, it is associated with the rate of decrease in solubility of the TAGs with the polarity increase [49].

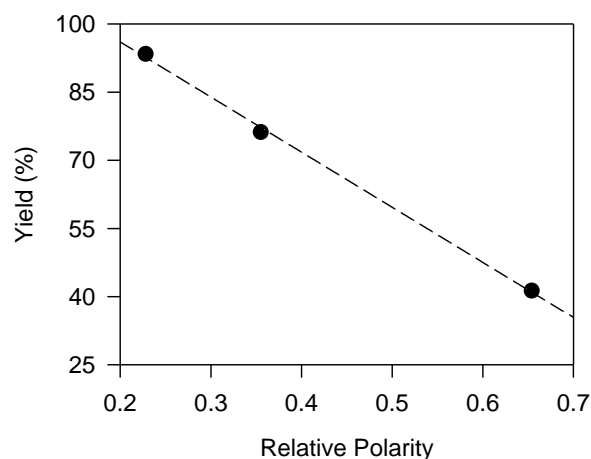


**Figure 2.** Yields of the soluble fractions in ethyl acetate, acetone and ethanol versus relative polarities. Dashed line is a fit to a straight line ( $R^2 = 0.998$ ).

The pKa values (see Table 2) strongly correlate negatively with the polarities of the solvents ( $r = -0.9954$ ), which provides a similarly strong but positive correlation with the fractionation yields and physical properties.

### 3.2. Chemical Analysis—Assessment of the Lipids of CWO and Its Fractions

The ESI-MS spectra of CWO and its fractions are provided in the Supporting Information (SI) in Figure S1. An example, the ESI-MS spectrum of CWO, is shown in Figure 3.

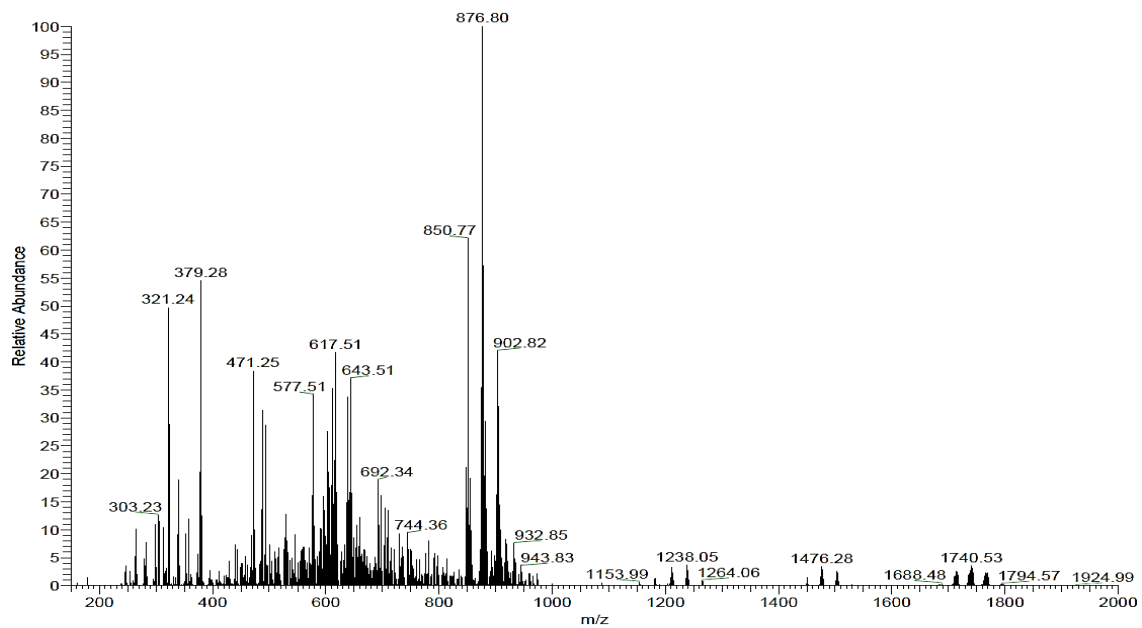


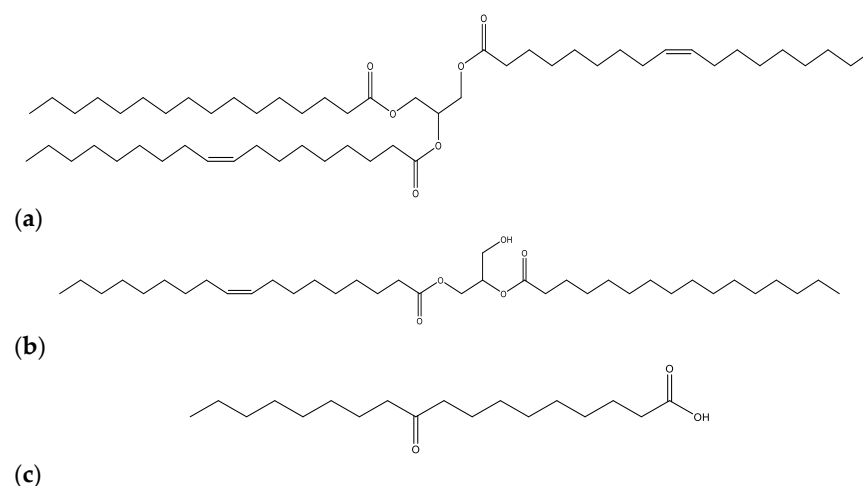
**Figure 3.** ESI-MS spectrum of crabwood oil (CWO). Analysis in QExactive Orbitrap mass spectrometer via direct injection, positive mode and scanning for two minutes. Image generated from the average of 1570 scans in Thermo Xcalibur software., version 3.1.

The lipid and non-lipid (non-saponifiable) compounds of CWO and its fractions were identified using MetaboQuest [50] and LIPID MAPS [51]. The relative abundances of the putative compounds were determined considering  $m/z$   $[M + Na]^+$ , which is, typically in the field, the most dominant adduct [52]. The abundance and distribution of individual compounds were assessed relative to their class rather than to the total lipids or non-lipids. The differences between the fractions expressed in relative abundances for each class of lipids were measurable and depended on the crystallization behavior and solubility of the lipids in the solvents. The MS results for the lipids and non-lipids are provided in Tables S1 and S2, respectively.

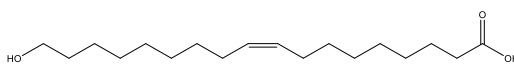
### 3.2.1. Assessment of the Lipids

The following four (04) classes of lipids were detected: TAG, DAG and occurring FFAs. The lipid assessment corresponds to the literature [52,53].

The chemical structures of the most abundant lipids detected in CWO are shown in Scheme 1.



**Scheme 1.** Cont.



(d)

**Scheme 1.** Representative molecules detected in the lipid group. (a) Palmito- diolein (PO<sub>2</sub>), the predominant TAG detected in CWO via ESI-MS, (b) 1-oleoyl-2-palmitoylglycerol, the predominant DAG detected in CWO via ESI-MS, (c) Predominant FFA detected in CWO via ESI-MS (c) 10-oxooctadecanoic acid (10-Ketostearic acid), (d) (Z)-18-hydroxyoctadec-9-enoic acid (18- hydroxyoleic acid).

#### Assessment of the Triacylglycerols

Seventeen (17) different TAGs were identified in CWO and in the fractions. Palmitic (P: C16:0) and oleic (O: C18:1) fatty acids account for about 60% of the total fatty acid composition of the TAGs. Because MS does not discriminate between positional isomers, the TAGs were identified without specification of the fatty acids position on the glycerol backbone. TAG symmetry is an important factor when considering crystallization; however, disregarding *sn*-2 acyl migration, which can occur depending on processing, temperature and time, mono- and di-unsaturated symmetrical or asymmetrical TAGs in CWO may be like those of palm oil, which occur in constant relative proportion [54]. No attempt was made to determine the relative proportion of symmetrical to asymmetrical TAGs in the samples. The relative abundances of the identified TAGs in CWO and its fractions are presented in Figure 4. The calculated molecular weight based on the TAG analysis is provided in Table 3.

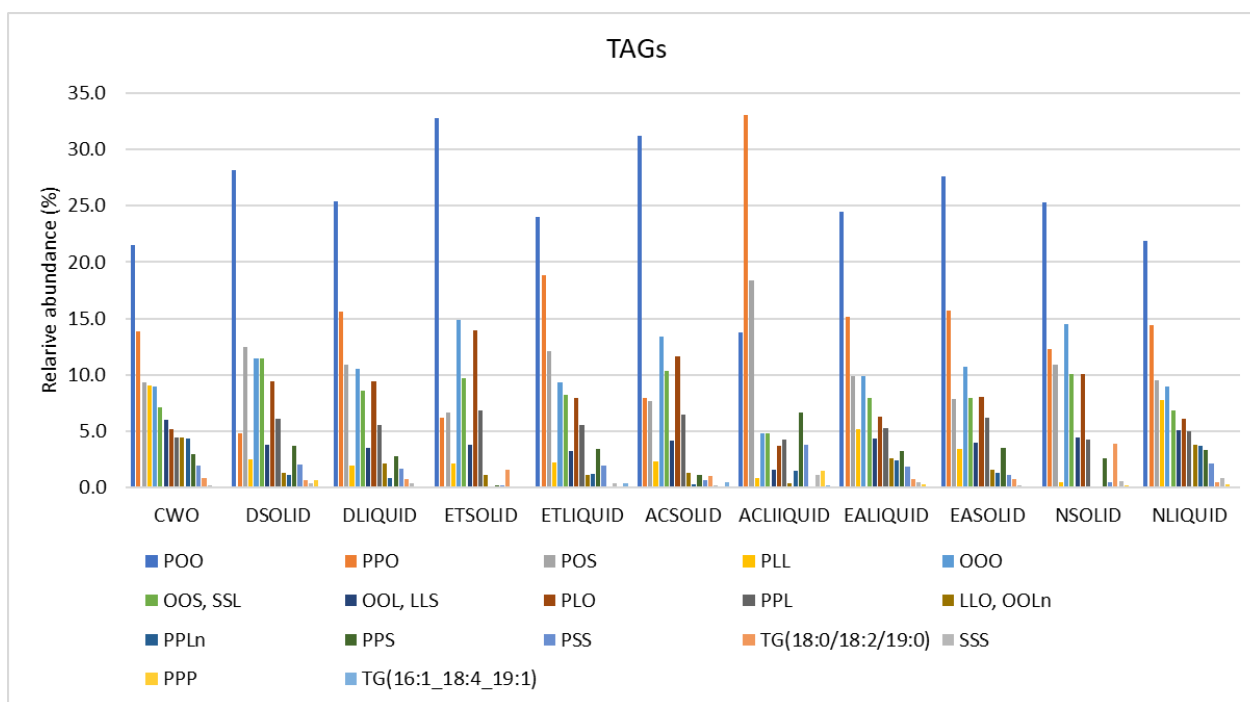


**Figure 4.** Relative abundance sorted in the descending order of TAGs in CWO and its fractions from dry and solvent (ethanol, acetone and ethyl acetate) fractionations. Abundances determined from the relative intensities of the ESI-MS sodium adducts.

The assessed TAG composition of the crabwood oil is within the ranges reported in the literature [52,53]. The main TAG in CWO is palmito- diolein (PO<sub>2</sub>: 21.5%) followed by oleo- dipalmitin (P<sub>2</sub>O: 13.8%). Except for AC<sub>LIQUID</sub>, in which P<sub>2</sub>O was prevalent (33.0% of the total), the main TAG detected in CWO and its fractions was also PO<sub>2</sub>. The relative abundance of PO<sub>2</sub> was maximum in ET<sub>SOLID</sub> with 32.8% of the TAGs and minimum in AC<sub>LIQUID</sub> with 13.7%.

**Table 3.** Calculated molecular weight based on this analysis.

Sample	MW (g/mol)
CWO	858.8
DSOLID	862.1
DLIQUID	859.1
ETSOLID	863.7
ETLIQUID	857.1
ACSOLID	862.5
ACLIQUID	850.0
EA LIQUID	858.4
EA SOLID	858.5
NSOLID	863.0
NLIQUID	858.2

To better clarify the partitioning, the TAGs are classified according to their saturation as follows: tri-saturated ( $S_3$ ), mono-unsaturated ( $S_2U$ ), di-unsaturated ( $SU_2$ ) and tri-unsaturated ( $U_3$ ). The main components of each group and their relative distribution may be emphasized to elucidate the differences in behavior between the fractions. Generally, stero-dipalmitin ( $P_2S$ ) is the main trisaturated TAG, whereas oleo-dipalmitin ( $P_2O$ ), palmito-diolein ( $PO_2$ ) and triolein ( $OOO$ ) are the most abundant TAGs of the  $S_2U$ ,  $SU_2$  and  $U_3$  classes, respectively. Figure 5 shows that the fractions are particularly enriched or depleted in  $S_3$ ,  $S_2U$ ,  $SU_2$  or  $U_3$ .

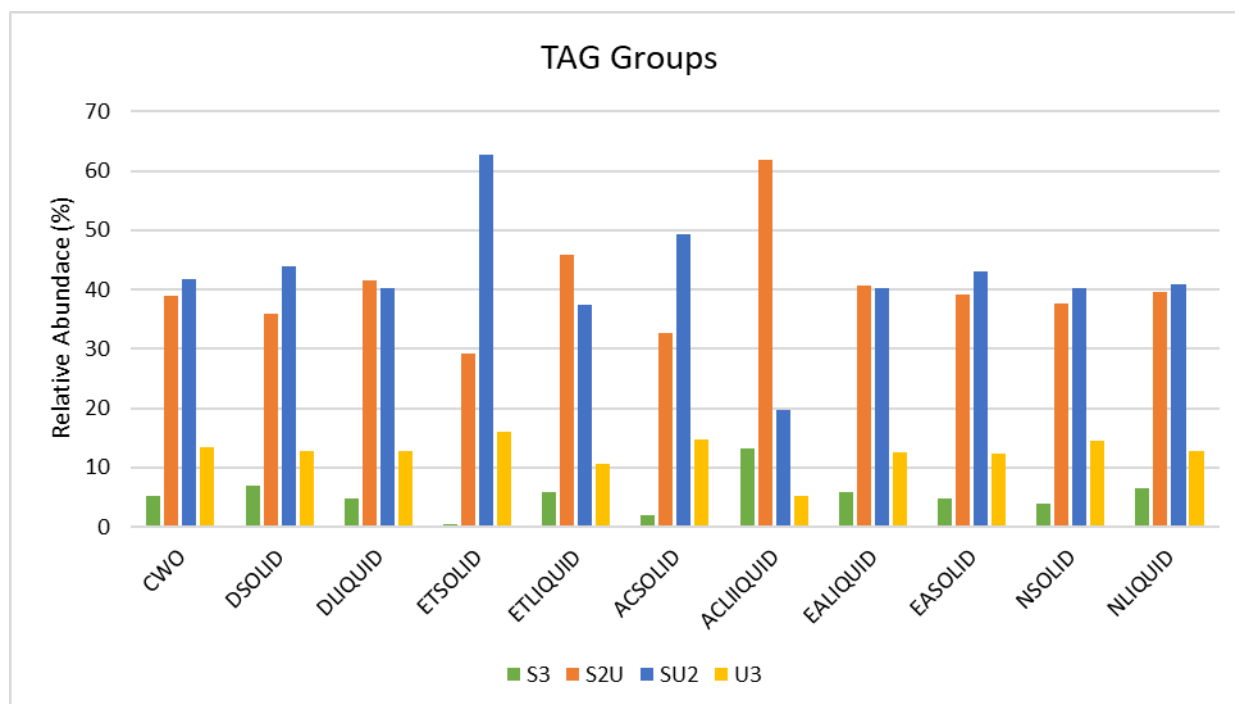


**Figure 5.** Distribution of tri-saturated ( $S_3$ ), mono-unsaturated ( $S_2U$ ), di-unsaturated ( $SU_2$ ) and tri-unsaturated ( $U_3$ ) TAGs detected in CWO and its fractions. Relative abundances determined from the relative intensities of the ESI-MS sodium adducts of the TAGs.

The distribution of the different groups between the solid and liquid fractions ranges from equivalent to twice larger depending both on the crystallization behavior of the TAG

systems and solubility in the case of solvent fractionation. The dry fractionation enriched the solid fraction in  $S_3$  and  $SU_2$  and depleted it of  $S_2U$ . The fractionation with ethyl acetate distributed each TAG group almost evenly in the solid and liquid fractions.  $ET_{LIQUID}$  and  $AC_{LIQUID}$  were significantly enriched in  $S_3$  and  $S_2U$  and depleted of  $SU_2$  and  $U_3$ , indicating a distribution dominated by solubility effects.

#### Assessment of the Diacylglycerols and Monoacylglycerols

The most abundant MAG detected in CWO and its fractions is monoolein (O), followed by monolinoleate (L). The most abundant DAG is 1-oleoyl-2-palmitoylglycerol (PO) followed by diolein (OO) in all the samples (Table S1b).

Noticeably, except for the ethyl acetate fractionation, which enriched the solid fraction in 8 of the 13 DAGs, the fractionations either distributed evenly or enriched the olein fractions by an average of 1.5 of most DAGs.  $EA_{SOLID}$  was also enriched with MAGs by an average of 1.5 times compared to  $EA_{LIQUID}$ . The distribution of TAGs and these data indicates that the fractionation with ethyl acetate separated the molecules more along the lines of polarity, particularly the DAGs and MAGs components, rather than saturation.

#### Assessment of the Free Fatty Acids

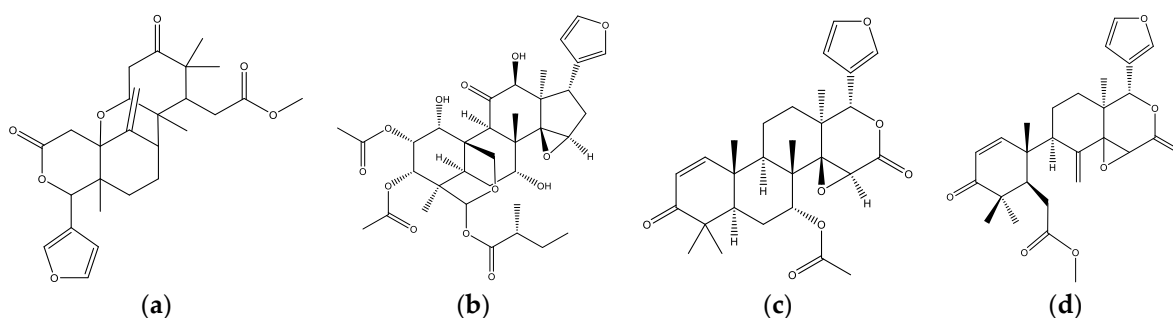
Fourteen FFAs were detected in CWO and its fractions. Saturated FFA in CWO accounts for 36% of the total FFA. The molecular mass sodium adducts ( $m/z[M+Na]^+ = 321.2408$ ) corresponding to both 10-oxooctadecanoic acid (ketostearic acid) and ((Z)-18-hydroxyoctadec-9-enoic acid (hydroxyoleic acid) were detected as the most abundant (43.7% of the total FFA). The two compounds cannot be discriminated with MS. These long fatty acids occur naturally, but to the best of our knowledge, they have not been reported in CWO before. They are essential nutrients and are known to play an important role in energy metabolism regulation [55]. Ketostearic acid is found in *Aloe ferox*, *Gracilaria longissima* and *Galeopsis bifida* [56], and 18-hydroxyoleic acid in *Arabidopsis thaliana* [57]. The presence of ketostearic and hydroxyoleic acids in CWO may be a result of the transformation that occurs during the fractionation process, or they might be specific to the Guyanese species of *Carapa guianensis* or even due to biotransformation by bacteria present in the Guyanese *Carapa guianensis*. The biotransformation of polyunsaturated fatty acids by gut lactic acid bacteria—such as linoleic acid to hydroxy fatty acids and other long-chain fatty compounds—is well-documented [58]. The origins, possible enhancement and separation of these fatty acids should form the basis of additional research in CWO.

The second most abundant FFA (24%) is 15-hydroxyoctadecanoic acid (hydroxy stearic acid). The relative abundance of linoleic acid is notable, with 11.2% of the total FFA. Linoleic acid is an omega-6 fatty acid parent compound of omega-6 fatty acids, such as  $\gamma$ -linolenic acids (GLA) and arachidonic acid [59] and omega-3 fatty acids, such as  $\alpha$ -linolenic acid (ALA) [60].

As the pKa increased, and because of increased solubility, the soluble fractions were increasingly enriched in weak acids, such as free fatty acids. The role of the pKa although prominent and the results can further enhance the design of specialized fractions, is more complex and needs further research work, particularly in the case of limonoids, and other bioactive compounds.

#### 3.2.2. Assessment of the Unsaponifiable Compounds

The non-lipids (unsaponifiable) compounds detected in CWO and its fractions consisted of 20 limonoids (Table S2a), seven sterols (Table S2b), one flavonoid, one tocopherol, one diterpenoid and one phosphoglycerol, labelled together “other unsaponifiable compounds” (Table S2c). These compounds have been reported in other plants of the Meliaceae family [61,62]. The chemical structures of the most abundant limonoids detected in CWO are shown in Scheme 2.



**Scheme 2.** Representative molecules detected in the limonoid group: (a) Methyl Angolensate, (b) Trichilin A, (c) Gedunin and (d) Andirobin.

#### Assessment of the Limonoids

The portioning of the most abundant limonoids in CWO and its fractions is presented in Figure 6. As can be seen, the most abundant limonoid in the samples is methyl angolensate (from 28 to 39%) followed by Trichilin A (from 13% to 22%). The angolensates are noteworthy because of their demonstrated cytotoxic [63,64] and antifungal [62,65] activities. Trichilin A is a limonoid reported to have important bioactivity, such as cytotoxic and antifeedant properties. Antifeedants are natural compounds produced by the plant to prevent the attack of pests, such as *Spodoptera eridania* (Southern armyworm), which feeds heavily on the leaves of young plants [66,67]. Although methyl angolensate has been reported in CWO [68], Trichilins have not, even though they have been identified in other Meliaceae species, such as Natal mahogany (*Trichilia roka*) [69]. The relative abundance of methyl angolensate and Trichilin A is large enough to warrant further investigation because of potential applications related to their bioactivities.

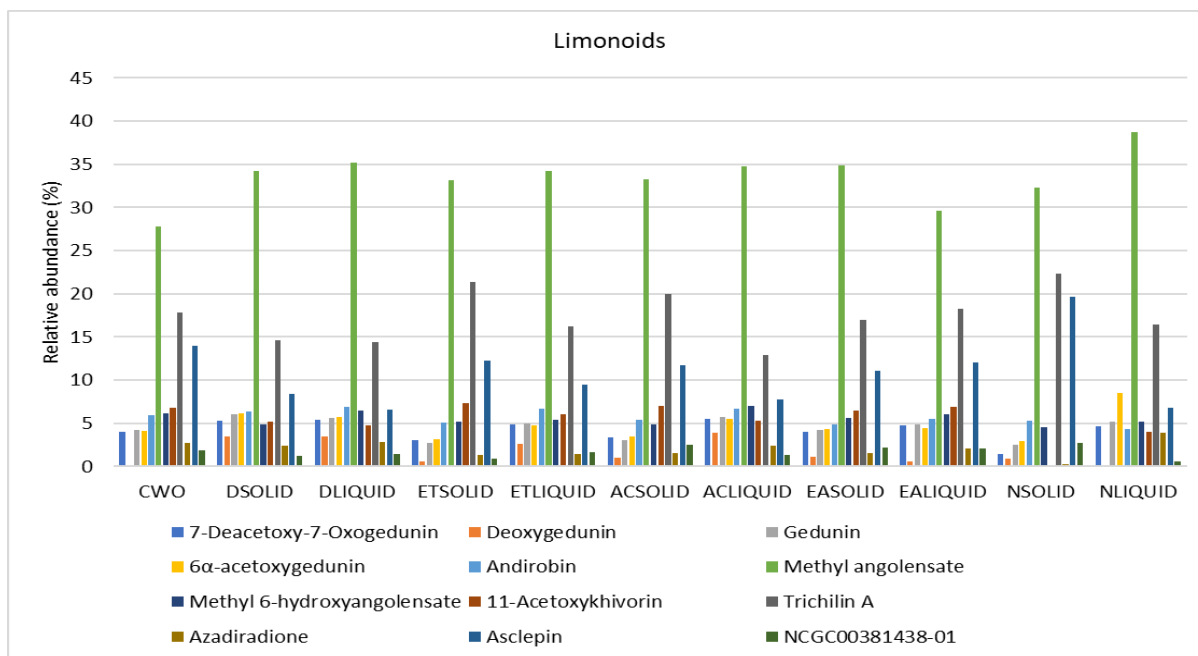


**Figure 6.** Distribution of the most abundant limonoids in CWO and its fractions. Relative abundances determined from the relative intensities of the ESI-MS sodium adducts of the limonoids.

The Andirobin and Gedunin class compounds are known for their antimicrobial activities, including antifungal, antibacterial, antifeedant, insecticidal, antimalarial, anti-allergic, anti-inflammatory, anti-cancer, anti-diabetic and neuroprotective activities [70,71]. Figure 6 shows that 7-deacetoxy-7-oxogedunin and Andirobin are the most predominant in all the fractions. The analysis of the relative abundances indicates that one can partition important

unsaponifiable compounds as a function of the fractionation method; in particular, there is a direct dependence on solvent polarity. Gedunin and Andirobin, for example, were more abundant in the liquid fractions. The correlation between polarity and Gedunin and Andirobin abundances was negative ( $r = 0.957$  and slope =  $-81\%$  per unit, and  $-0.991$  and slope =  $-27\%$  per unit, respectively, Figure 7).

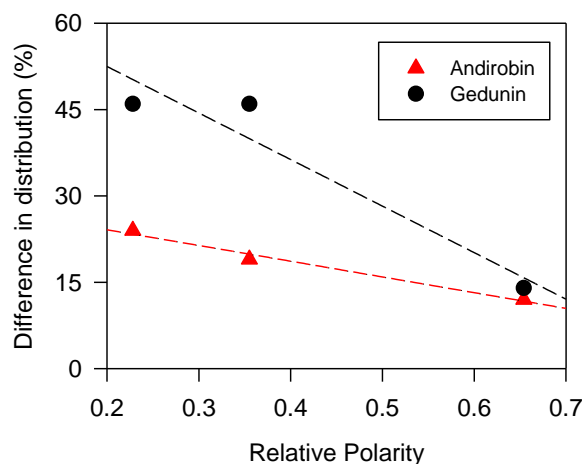


**Figure 7.** Difference in distribution of Gedunin and Andirobin between the olein and stearin fractions obtained from ethyl acetate, acetone and ethanol fractionations versus relative polarities. Dashed lines are fits to straight lines ( $R^2 = 0.982$  and  $0.916$  for Andirobin and Gedunin, respectively).

The Carapanolides, which were in low amounts (less than 1.3%), were more present in the olein fractions. The other putative limonoids listed in Table S2 have been reported in other plants of the Meliaceae family [61,62]. The partitioning of these compounds between the stearin and olein fractions obtained from the solvent was significant. The distribution of these limonoids depended on the type of solvent used, but no correlation was found with the polarities.

#### Assessment of the Sterols

Seven sterols were identified in CWO. 2-Deoxy-20-hydroxy-5 $\alpha$ -ecdysone 3-acetate was the most prevalent in CWO (18%) in all the fractions and is similarly abundant in the olein fractions and the dry stearin ( $\pm 0.6\%$ ). This sterol belongs to a class called ecdysteroid esters found effective for anti-cancer activity [72].

#### Assessment of the Other Unsaponifiable Compounds

The most dominant compound of the group is the phosphoglycerol, which accounts for 36% of the total. Its distribution did not vary significantly between the stearin and olein fractions obtained by the dry fractionation methods ( $\pm 2\%$ ), whereas the stearin fractions obtained by ethyl acetate, acetone and ethanol expressed 3%, 17% and 11% more phosphoglycerol, respectively. The differences observed for the flavonoid and the tocopherol were not statistically significant.

As pKa increased and because of increased solubility, the soluble fractions were increasingly enriched in weak acids, such as free fatty acids. The role of pKa although prominent, its role is more complex and needs further research, particularly for the limonoids, and other bioactive compounds.

#### 3.3. Thermal Transition Behavior

The cooling (5 °C/min) and heating (10 °C/min) thermograms of CWO and its fractions are shown in Figure 8(a1–2) and (b1–2), respectively. The corresponding crystallization and melting data are provided in the SI in Table S2 and Table S3, respectively.

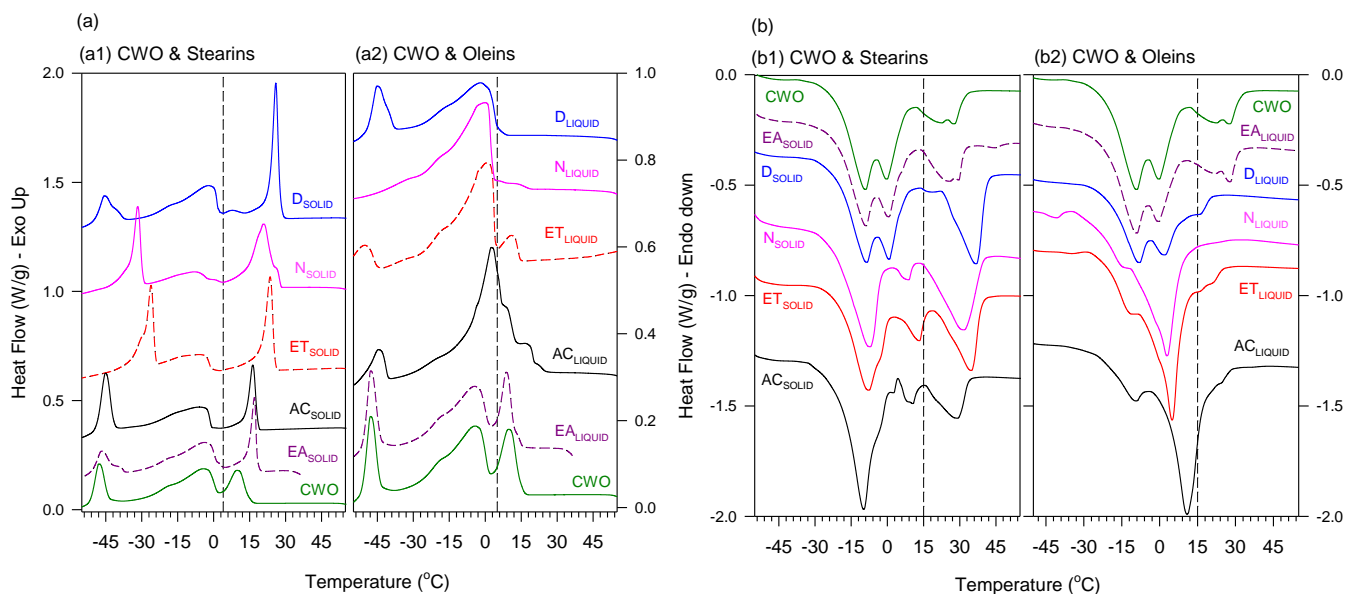


**Figure 8.** (a) Cooling (5 °C/min) and (b) heating (10 °C/min) DSC thermograms of CWO and its stearin and olein fractions. Dashed lines separate the high- and low-temperature thermal transition zones.

The cooling thermogram of CWO is characterized by a relatively sharp high temperature leading event  $T_{C1}$  at 11.4 °C and two prominent subzero exotherms (−3.4 and −47.4 °C, Figure 8(a1–2)), indicating high, medium and low melting components. The high melting group of molecules distinctly separates from the low melting groups at 4 °C, indicating the possibility of fractionating CWO into a stearin fraction (SOLID comprising mostly high melting TAG components) and an olein fraction (LIQUID mainly comprising the mid and low melting TAG components).

The DSC thermograms of the CWO fractions are altered versions of CWOs. The enrichment of the stearin fractions in the saturated components ( $S_3$ ) manifested in the high temperature leading exotherms, whereas the corresponding depletion of the olein fractions in these elements manifested as a weaker or even absent high temperature leading peak. The transformation paths recorded during heating included recrystallizations mediated by melting and resolved endotherms, indicating there was a melting of different crystal phases.

### 3.3.1. Crystallization Behavior

The stearin fractions comprised the two subzero crystallization peaks (Figure 8(a1)), indicating the presence of liquid phases. The stearin fractions presented leading events at temperatures higher than CWO ( $T_{C1} = 11.4$  °C), with  $D_{SOLID}$  presenting the highest (26 °C) followed, in order, by the following:  $ET_{SOLID}$  at 23.5 °C,  $EA_{SOLID}$  at 17.0 °C and  $AC_{SOLID}$  at 16.3 °C. Conversely, in that range of temperatures, the olein fractions had smaller or even, like  $D_{LIQUID}$ , absent peaks above 3 °C (Figure 8(a2)). The leading peaks of  $EA_{LIQUID}$  (9.0 °C) and  $ET_{LIQUID}$  (11.0 °C) are similar to those of CWO, whereas  $AC_{LIQUID}$  presented four distinct but non-resolved exotherms (23, 17, 9 and 3 °C).

The soluble components from solvent fractionation gradually lose their stearin character as the polarity decreases from ethanol to acetone ( $ET_{LIQUID}$  and  $AC_{LIQUID}$ ) and become an olein for ethyl acetate ( $EA_{LIQUID}$ ; Figure 8(a1–2)). The cooling thermograms of  $EA_{SOLID}$  and  $EA_{LIQUID}$  are like CWO in shape, but they present differences in peak temperatures and enthalpies. The leading exotherm associated with  $EA_{LIQUID}$  (9.0 °C,  $\Delta H_{c1} = 12$  J/g) is only slightly lower than that of CWO (~11.4 °C,  $\Delta H_{c1} = 13$  J/g), indicating a close saturation distribution. Both are significantly lower than  $EA_{SOLID}$  (17 °C,  $\Delta H_{c1} = 27$  J/g). The enrich-

ment of  $EA_{SOLID}$  with most of the DAGs, known to act as seeds for early crystallization, may explain the high crystallization peaks.

The enthalpies of the stearin fractions can be associated with a solid fat content. Overall, as shown in Figure 9a,b, the enthalpy of crystallization of the leading event for the stearin fractions ( $\Delta H_{1s}$ ) was much higher than that of the olein fractions ( $\Delta H_{1o}$ ).

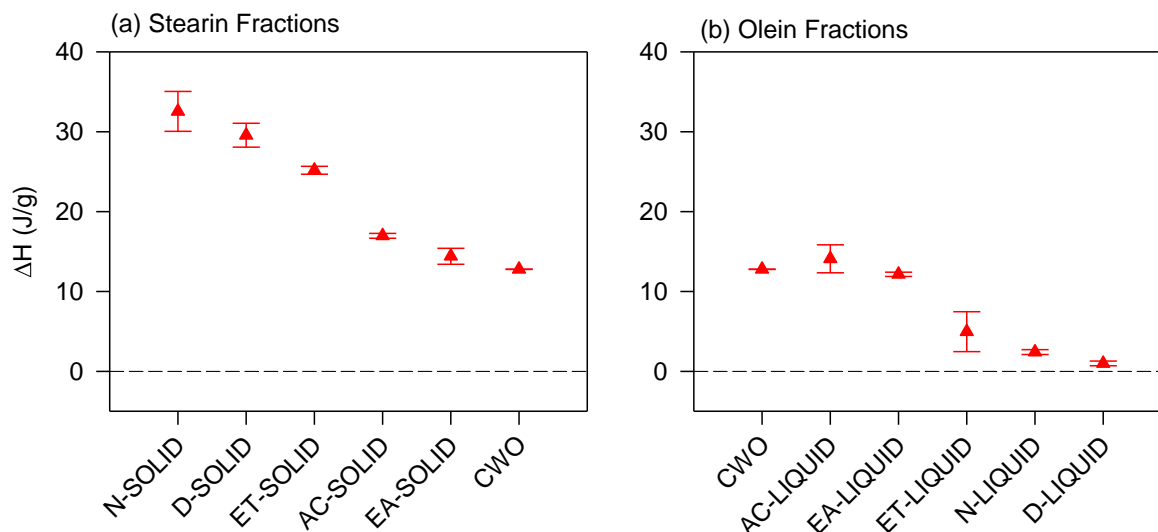


**Figure 9.** Enthalpy of crystallization from DSC of the leading peak ( $\blacktriangle$ ) of the (a) stearin and (b) olein fractions of CWO.

Note that  $\Delta H_{1o}$  of  $ET_{LIQUID}$ ,  $N_{LIQUID}$  and  $D_{LIQUID}$  are the lowest ( $<4 \pm 3$  J/g). The differences in the intensity of the leading peaks are caused by the fractionation method, and solvent polarity and this is measurable, hence, the olein fractions, which reflect the depletion of the most saturated components, can be used to assess the relative separation efficiency of the fractionation methods.

The correlation between  $\Delta H_{1s}$  and the relative polarity of the solvents is strong and statistically significant ( $r = 0.9979$ ; Figure 10). The slope of the correlation line  $25.7 \pm 1.7$  J/g per relative unit is a quantification of the effect of polarity on the partitioning of the lipids, which can be used to control fractionation and select specific solid and liquid fractions of CWO by solvents.

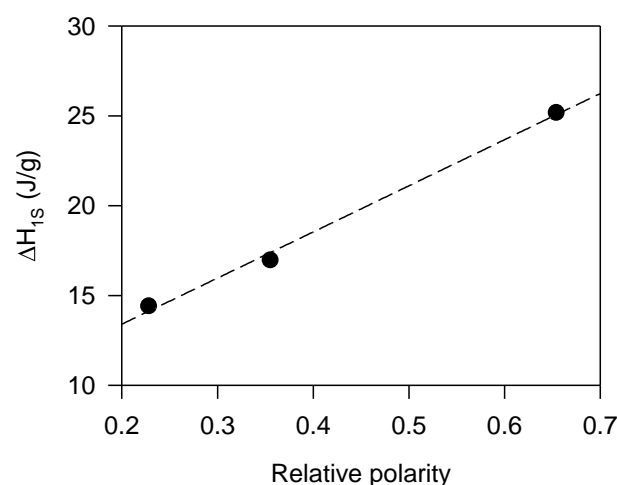


**Figure 10.** Enthalpy of crystallization from DSC of the leading peak of the stearin fractions ( $\bullet$ ) obtained by ethyl acetate, acetone and ethanol fractionations versus relative polarities. Dashed line is a fit to a straight line ( $R^2 = 0.996$ ).

### 3.3.2. Melting Behavior

The heating thermograms of the stearin fractions are characterized with four main endotherms (Figure 8(b1)), and, except for EA<sub>LIQUID</sub>, those of the olein fractions were missing the highest temperature melting peak ( $T_{m1}$ ) (Figure 8(b2)). This indicates that the most stable phases generally available for CWO did not form in the olein fractions.

The most stable phases of the stearin fractions, as indicated by their  $T_{m1}$ , were markedly different.  $T_{m1}$  of EA<sub>SOLID</sub> (44.4 °C), D<sub>SOLID</sub> (36.7 °C) and N<sub>SOLID</sub> (31.2 °C) were higher than  $T_{m1}$  of CWO (27.6 °C), AC<sub>SOLID</sub> (23.4 °C) and ET<sub>SOLID</sub> (19.5 °C). This decrease in  $T_{m1}$  mirrors the trend observed for the leading crystallization event indicating that it was those crystals formed during cooling that transformed and melted. The significant differences in  $T_{m1}$  (up to 23.9 °C) can be associated with the partitioning of the most saturated elements, including the saturated and di-saturated TAGs, as well as the minor lipid components and the non-saponifiable components. The prominent peaks observed at  $0 \pm 2$  °C and  $-10 \pm 2$  °C indicate that the same low-temperature crystal phases occur in all the fractions. Despite being overwhelmed by the endotherms, recrystallizations mediated by melt are evident in the heating thermograms of all the samples. This is a common occurrence in fats and oils [73].

The heating thermogram of the fractions from ethyl acetate is singular. EA<sub>LIQUID</sub> displayed four melting events, of which the highest at  $T_{m1} = 23.4$  °C indicates a lower stability phase than that of CWO. EA<sub>SOLID</sub> shows six distinct melting events, including a large endotherm at 27.6 °C, which matches the highest of CWO (27.6 °C). A small endotherm shows in EA<sub>SOLID</sub> at 44.4 °C, probably because of the sizable amounts of saturated FFAs and DAGs.

### 3.3.3. Thermal Transition Behavior and Lipid Profile

The categorization into different saturation groups (Figure 5) helps explain the behavior of CWO and its fractions. The behavior of these complex palmitic/oleic TAG systems is generally dictated by the behavior of the main components and their interactions. The influence of fatty acid unsaturation is critical, driving the properties in both metastable and stable forms [74,75]. The main components of the different saturation groups, namely, P<sub>2</sub>S, P<sub>2</sub>O, PO<sub>2</sub> and OOO form binary and higher-order systems with specific interactions through the acyl chains leading to the formation of particular transition behaviors, including monotectic behavior, eutectics and molecular compounds. These systems that contain palmitic and oleic acids are relatively well-studied [76].

Table S1 shows that the solid fractions (stearin) are particularly enriched in S<sub>3</sub> compounds at the detriment of the liquid fractions. Although the stearin fractions were depleted in S<sub>2</sub>U (P<sub>2</sub>O being the most abundant), a sizable amount remained, which suggests that it played an essential role with the TAGs of S<sub>3</sub> (PSS/PPS/PPP) in the physical characteristics of the CWO fractions. A minimal amount of PPS in the olein fractions seems necessary for their crystallization. The tendency of POP, POO, OPO, OPP and POP blends to form molecular compounds, which release significant heat when crystallizing, can explain the typical crystallization behaviors of the olein [76].

### 3.4. Solid Fat Content

The SFC versus time curves of CWO and its fractions from the in situ step and isothermal measurements followed an exponential rise to a maximum ( $SFC(T) = SFC_0 + a(1 - \exp(-t/t_0))$ ;  $R^2 > 0.8625$ ). The final SFC obtained at 25, 18, 10 and 0 °C is shown in Figure 11.

The SFC of the liquid fractions was much smaller than those of the solid fractions above 4 °C. The SFC of the fractions obtained at 25 °C was not significantly different ( $p < 0.05$ ), averaging  $7 \pm 1\%$  for the stearins and 3% for the oleins. Below 25 °C, AC<sub>SOLID</sub> achieved the highest SFC (19% at 18 °C and 36% at 0 °C) and ET<sub>SOLID</sub> the lowest (10% at 18 °C and 12% at 0 °C). D<sub>SOLID</sub> and N<sub>SOLID</sub> achieved similar SFCs (12% at 18 °C and

15% at 0 °C). The SFC of the liquid fractions increased substantially at 0 °C, indicating the involvement of molecules of a higher unsaturation.

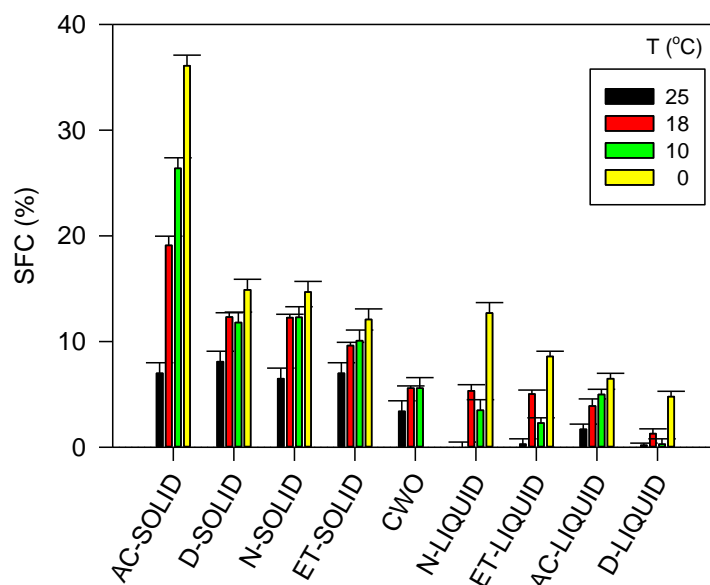


**Figure 11.** SFC of CWO and its fractions measured by pulsed NMR at (25, 18, 10 and 0) °C.

The understanding gained from the crystallization behavior of palmitic-oleic TAGs is applied here to explain the SFC at the different temperatures. The main groups of molecules, which are susceptible to crystallizing above 4 °C, are those comprising the most saturated components, such as the saturated PS<sub>2</sub> and P<sub>2</sub>S and their interaction with the di-saturated TAGs, such as P<sub>2</sub>O. At the freezing temperature, the crystallization of the di-unsaturated TAGs, such as PO<sub>2</sub>, PLO and PL<sub>2</sub> (which together form approximately 43% of the TAGs of CWO), may be involved in a significant manner.

The detailed examination of N<sub>LIQUID</sub>, N<sub>SOLID</sub> and D<sub>SOLID</sub> presented in Figure 12, indicates important differences in the evolution of the SFC due to different crystallization kinetics. The SFC versus temperature curves of N<sub>LIQUID</sub> (Figure 12a) and D<sub>SOLID</sub> (Figure 12c) show two distinct segments, indicating a two-step crystallization process. This indicates that the crystallizations of the most saturated components and the mid melting components occur separately when processed in the MNR machine, similar to what is observed in the DSC between the leading crystallization exotherm and the exotherm at  $T_{c2} = -2$  °C.

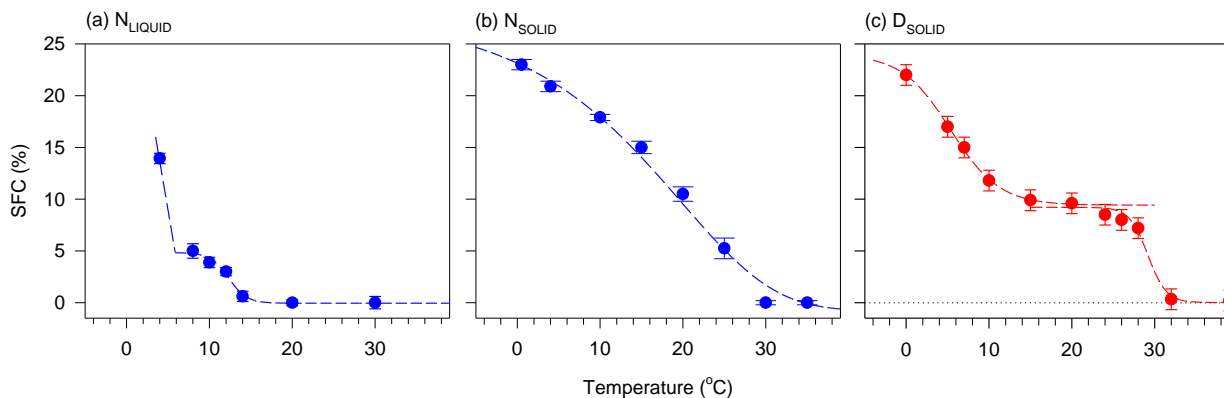


**Figure 12.** SFC measured by pulsed NMR versus temperature of the solid fraction obtained by dry fractionation of CWO (D<sub>SOLID</sub>) and the solid and liquid fractions obtained by decanting CWO (N<sub>SOLID</sub> and N<sub>LIQUID</sub>, respectively).

Despite a crystallization path like  $D_{\text{SOLID}}$ , the SFC of  $N_{\text{SOLID}}$  displayed one sigmoidal segment, indicating different relative contributions of the activated secondary nucleation processes to the overall growth rate and apparent activation energies [77–79]. Measurements below freezing, which would show the contribution of the components of CWO, which crystallize at lower temperature ( $-35\text{ }^{\circ}\text{C}$ ), were not performed.

The role of kinetics in the SFC of CWO and its fractions is further evident from the measurements of the samples at  $4\text{ }^{\circ}\text{C}$  under two different thermal protocols (Figure 13). This is demonstrated by (a) cooling from the melt in small steps ( $2\text{ }^{\circ}\text{C}$ ) and isothermal measurement, and (b) after 8–10 days storage time. Protocol (a) resulted in a much higher SFC with gains varying from  $\sim 65\%$  ( $ET_{\text{LIQUID}}$ ) to  $14\%$  ( $AC_{\text{LIQUID}}$ ).

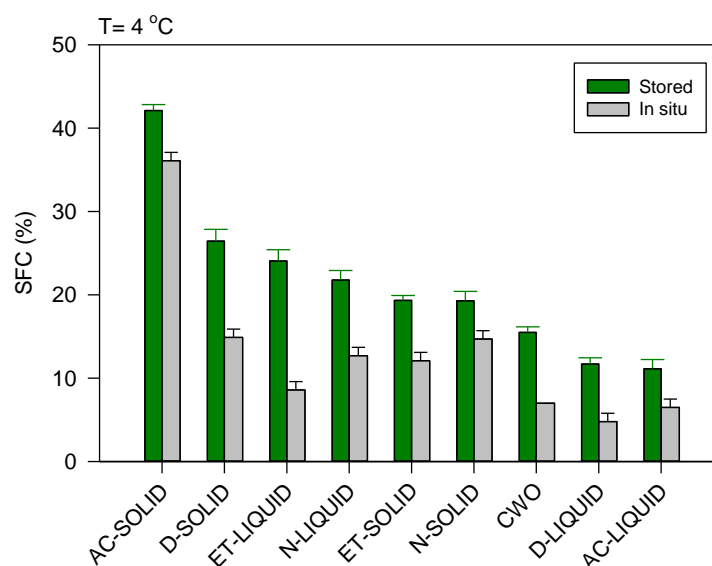


**Figure 13.** SFC measured by pulsed NMR at  $4\text{ }^{\circ}\text{C}$  of CWO and its fractions for samples (i) cooled in situ from the melt and measured isothermally in small steps ( $2\text{ }^{\circ}\text{C}$ ) and (ii) after an 8–10-day storage time.

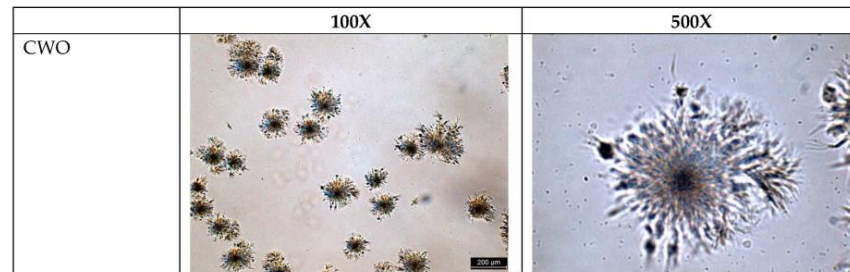
### 3.5. Microstructure of Crabwood Oil and Its Fractions

The PLM images of CWO (Figure 14a) show large spherulitic crystals of long radial dendrites dispersed in a sizeable liquid phase. The microstructures of both the stearin and olein fractions (Figure 14b,c) were significantly altered by the fractionation method and solvent used.  $EA_{\text{LIQUID}}$  (Figure 14c) displayed microstructures with crystals resembling those of CWO but with longer dendrites (250 nm vs. 175 nm on average) and much less liquid phase. The size of the crystals of all the other fractions was reduced to less than  $20\text{ }\mu\text{m}$ , and their number increased, indicating high nucleation and crystallization rates.

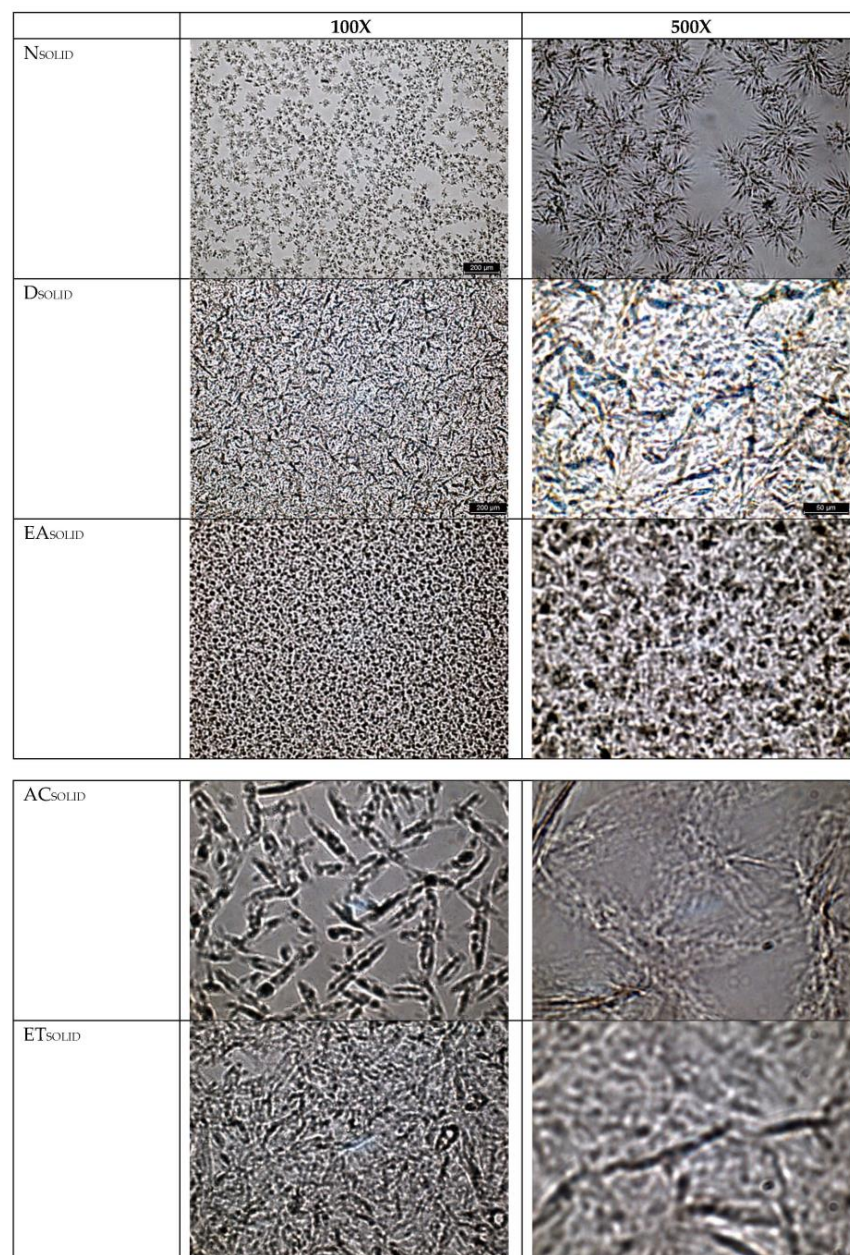
The crystals of the stearin fractions were either homogeneously distributed in relatively compact, dense networks in which the liquid phase is trapped ( $D_{\text{SOLID}}$ ,  $EA_{\text{SOLID}}$ ,  $ET_{\text{SOLID}}$ ; Figure 14b), or they were closely and homogeneously dispersed in a small liquid phase ( $N_{\text{SOLID}}$ ,  $AC_{\text{SOLID}}$ ; Figure 14b). The crystals of the olein fractions were all dispersed in a large liquid phase (Figure 14c).

The details of the microstructures, such as shape, size and distribution of the crystals of the different fractions, are measurably distinguishable. The sizes vary from 5 to  $250\text{ }\mu\text{m}$ . The shapes include well-organized spherulites, and needle-like and rod-like crystals. The distribution of the crystals varies from highly dispersed to compact networks. Because of the predominance of the liquid phase, the microstructures of the olein fractions differ measurably in all these parameters but in a more subtle manner than in the stearin fractions. The different microstructures of the stearin fractions depended on the solvent.  $EA_{\text{SOLID}}$  formed a dense network of small spherulitic crystals,  $AC_{\text{SOLID}}$  formed an open network of long (20 nm on average) rod-like crystals, whereas  $ET_{\text{SOLID}}$  comprised both types of

crystals organized in a dense network. The microstructures of the stearins from solvent also measurably differ from those obtained by dry fractionation ( $D_{SOLID}$  and  $N_{SOLID}$ ) in crystal type, size and distribution.

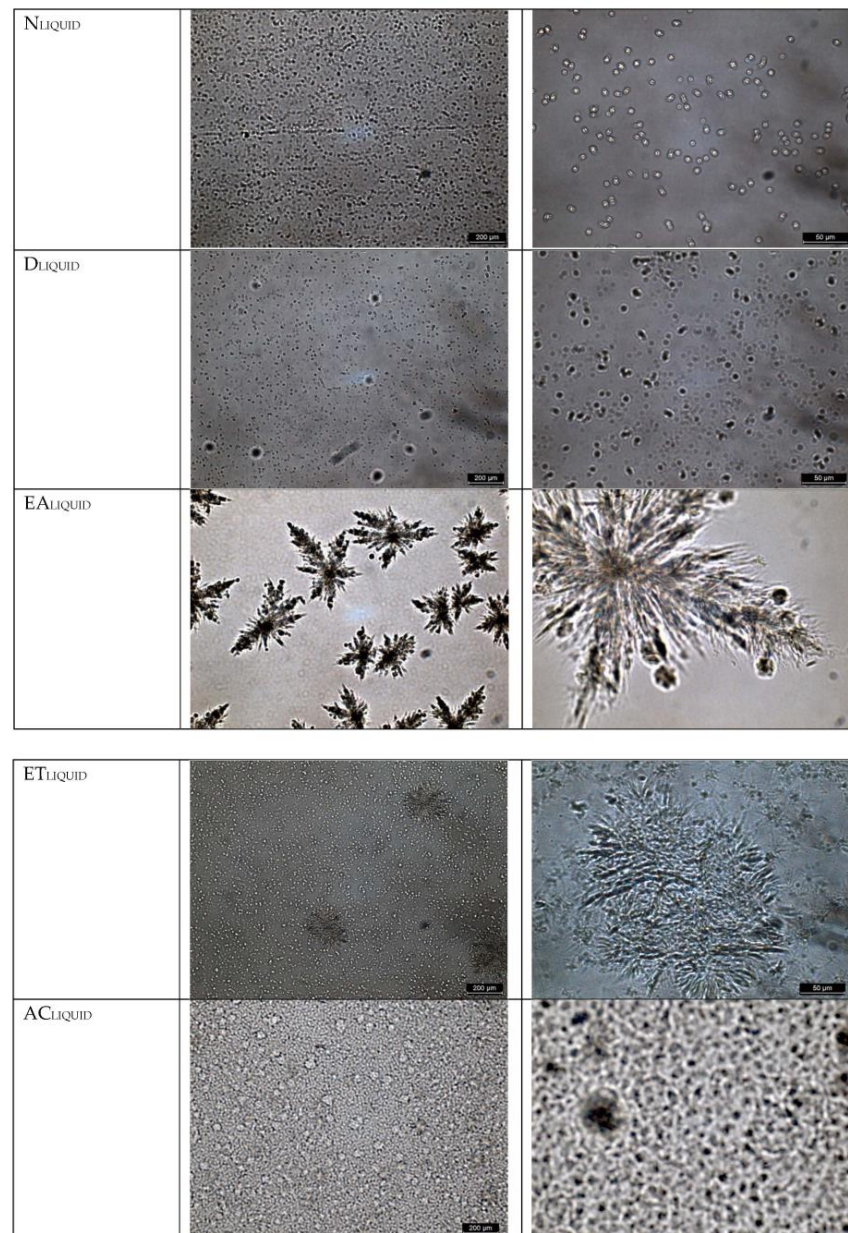


(a) CWO



(b) Stearin Fractions

Figure 14. Cont.



(c) Olein Fractions

**Figure 14.** PLM images taken after 7–10 days at room temperature (18 °C) of (a) CWO, and the (b) stearin fractions and (c) olein fractions obtained from dry, ethyl acetate, acetone and ethanol fractionations.

The diversity of the microstructures suggests that the fractions are likely to have different flow characteristics and different feels to the skin and mouth. This also suggests that they will confer different textures, consistencies and mouthfeels to fat products. This is often determined by both the shape and size of the crystals and aggregates, with the large microstructures promoting grainy texture [80]. The smaller crystals would lead to firmer products and larger size crystals to sandy mouth feel [81]. Their mechanical properties would be different because they are mostly controlled by the material's networks of polycrystalline microstructures and the SFC [82].

### 3.6. Crystal Structure of CWO, CWO Fractions

The XRD of the olein fractions did not present crystal peaks because of the overwhelming liquid phase. The normalized SAXD and WAXD spectra obtained for CWO and its

stearin fractions are shown in Figure 15. The d-spacings and the related Miller indices are provided in the SI in Table S1.

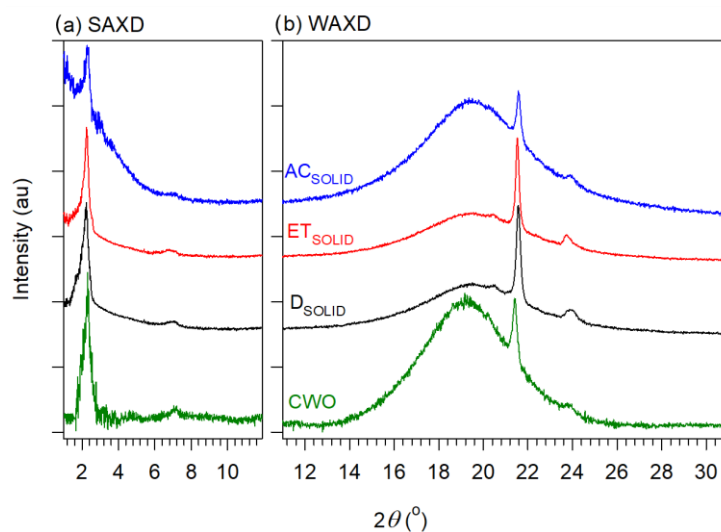


**Figure 15.** (a) Small-angle X-ray diffraction (SAXD) and (b) Wide-angle X-ray diffraction (WAXD) of crabwood oil (CWO) and its solid fractions. ET<sub>SOLID</sub>, AC<sub>SOLID</sub> and D<sub>SOLID</sub>: solid fractions obtained from acetone and dry fractionations, respectively.

CWO and its fractions presented their diffraction peaks at 4.16 Å (110) and 3.74 Å (200), a characteristic of an orthorhombic subcell structure in the  $\beta'$ -form and a substantial wide background halo at approximately 4.8 Å, indicative of the liquid phase in the sample. Their SAXD is consistent with the double chain length (DCL) packing in the fork configuration of TAGs containing predominantly C16 fatty acids. The C16-DCL packing reflects the predominance of CWO and its fractions of high melting temperature TAGs containing palmitic acids, such as PPS, PPO and POS.

### 3.7. Thermal Gravimetric Analysis

The TGA and DTG curves and the corresponding data of all the samples are provided in the (SI) in Figure S2 and Table S1, respectively. TGA and DTG curves representative of the solid, liquid, soluble and insoluble fractions are shown in Figure 16a and b, respectively.

The onset temperature of mass loss as determined at 5% ( $T_{5\%}^{on}$ ) of the stearin fractions (Figure 16c) are not significantly different ( $195 \pm 2$  °C). Also,  $T_{5\%}^{on}$  of AC<sub>SOLID</sub> and N<sub>LIQUID</sub> are not significantly different from CWO ( $205 \pm 2$  °C).  $T_{5\%}^{on}$  of the insoluble fractions increase with increasing solvent polarity.

Figure 16b indicates that the CWO fractions experience the same two main mass loss mechanisms ( $T_{D1} = 233 \pm 6$  °C and  $T_{D2} = 393 \pm 8$  °C). A small event showed centered at  $T_{D3} = 435.8$  °C but involved less than 2% of mass loss. The degradation of CWO and its fractions can be understood considering the mechanisms by which TAGs degrade, i.e., via  $\beta$ -hydrogen elimination starting at 250–380 °C and  $\gamma$ -hydrogen transfer starting at 450 °C [83–85].

The ~140 °C–300 °C range of the first DTG peak was identified as the range in which the volatilization of free fatty acids occurs. Niu et al. [86] reported that the gaseous products from the thermal degradation of oleic acid involve alkanes in large proportions, but also alkenes, aldehydes, ethers and CO<sub>2</sub>. It is safe to assume that all the free fatty acids and other minor light components were lost at ~300 °C, the offset temperatures of the first DTG peak. However, because the  $\beta$ -hydrogen elimination starts at ~240 °C, this peak may also involve the degradation of MAGs, DAGs as well as TAGs.

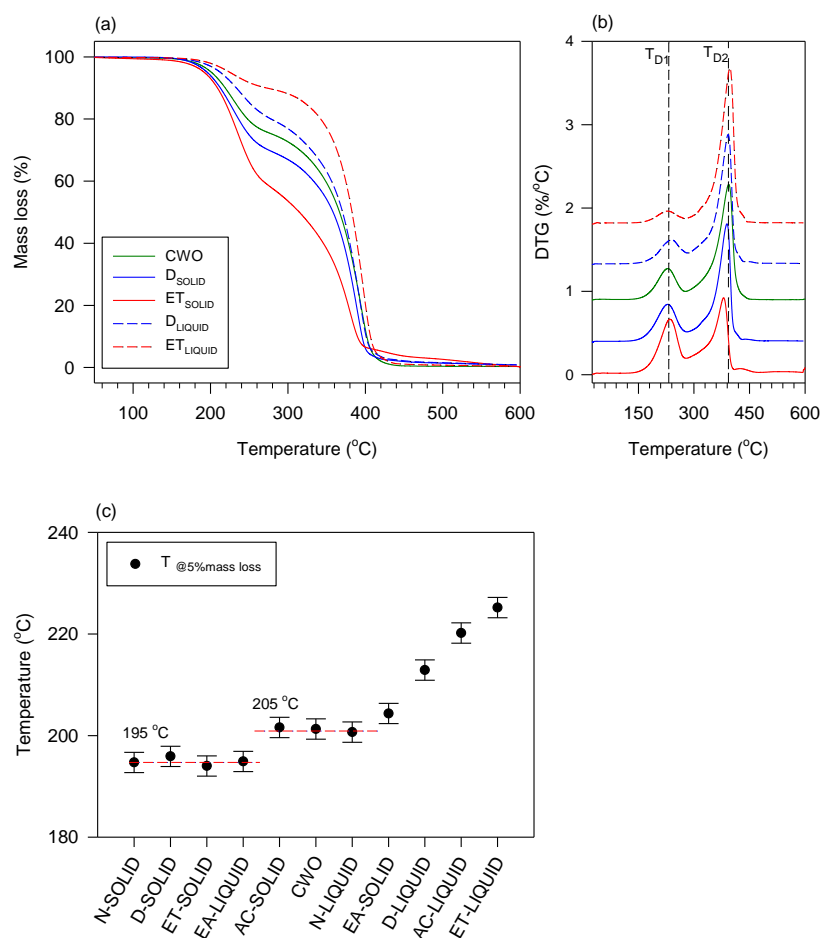


**Figure 16.** (a) TGA and (b) DTG stacks of crabwood oil (CWO) and its fractions from dry and ethanol fractionations; (c) onset temperature of degradation as determined at 5% mass loss ( $T_{5\%}^{on}$ ) of CWO and its fractions from dry, ethanol, acetone and ethyl acetate fractionations.

The 300–450 °C temperature range involves the degradation of the saturated as well as the unsaturated fatty acids of the TAGs, as has been reported to occur, such as in rapeseed oil [87] and virgin olive oil [88]. In a study of pure simple TAGs with C18:0, C18:1, C18:2 and C18:3 fatty acids, one DTG step was observed for C18:0, C18:2 and C18:3 and two partly separated steps were observed for C18:1, suggesting that it starts to degrade before all the other fatty acids [88].

#### 4. Conclusions and Perspectives

This work involves the study of the oil from the seeds of *Carapa guianensis*, known as crabwood oil (CWO) and its fractionation. The oil is composed of lipids (95–98%) and non-saponifiable compounds (2–5%) comprising limonoids, sterols and phenols. Dry and solvent fractionation with ethanol, acetone and ethyl acetate were used to obtain narrower composition ranges that have altered physical properties and meet specific functional requirements for use in the food, pharmaceutical and cosmetic industries. The established methods of phytochemical and physicochemical functionality analysis were used to determine the functionality of the fractions.

The fractionation work yielded stearin and olein fractions that have measurable and, in some instances, predictably significant differences in the studied chemical and physical characteristics that depend on the fractionation method and solvent polarity. A conclusion was supported that fractionation of CWO using solvents has great potential to be further directed by using other solvents, mixtures of solvents and by varying the process

parameters, such as solvent-to-oil ratio, crystallization temperature, agitation, cooling rate and crystallization time.

The work achieved the following important specific findings:

1. Fractionation resulted in a changed microstructure: the fractions displayed smaller crystals than CWO, which were distinguishable in shape, size and density of the crystal networks;
2. Fractionation changed the crystallization and melting temperatures: The partitioning of the lipids is significant enough to drive measurable and predictable crystallization and melting behaviors. The solid fractions transition parameters were particularly very strongly correlated to the fractionation method and polarity of the solvents;
3. Fractionation changed the solid fat content (SFC) profile of CWO fractions: CWO fractions are shown to form semi-solid fats. The role of kinetics is significant and manifests differently depending on the fractionation method and solvent polarity. The data suggest that it is possible to improve the SFC of the fractions by changing the processing methods;
4. One can tailor physical properties, such as crystallization, melt and solid fat content and possibly texture (through drastic modification of microstructure), through fractionation, using polarity as a predictive tool.

This work shows the potential to make unique compositions with significantly different properties through the fractionation of CWO by using polarity as a predictive tool. The olein fractions can be used to make improved emulsions, creams and salves with specific physical properties, with antimicrobial and antifungal efficacy due to the bioactive components of CWO. The stearin fractions can be used for specialized products desirable in topical cosmetic and pharmaceutical applications.

*Carapa guianensis* seed oil is important for Guyana. It is currently sold in local markets and pharmacies for its medicinal and cosmetic attributes. The reported methods would first provide high-value fractions with targeted enriched compositions suitable for developing materials with customized lipid and bioactive compositions. Bio-potent liquids and solid fractions would be valuable in specific pharmaceutical and cosmetic applications. The antimicrobial and antifungal compounds of CWO can be administered via adequate methods (liquid of fat) to fend off many diseases, such as malaria and vaginosis, endemic to Guyana and tropical countries. With proper safety measures, one can expect the emergence of strong and consequential Guyanese pharmaceutical and cosmetic sectors based on CWO and other similar oils. At a large scale, the less valuable products, if any, because of a potentially large supply, would possibly allow for the development of a more traditional oleochemical industry and a sustainable administration of this very valuable tree, which presently is heavily logged in Guyana.

The results call for further investigations and optimization, which would establish robust, predictable relationships between the processing conditions and the chemical structure and function. The study of other solvents/solvent mixtures and fractionation conditions (solvent-to-oil ratio, crystallization temperature, agitation, cooling rate and crystallization time) that affect the yield and quality can result in controlled narrower fractions and partition of both the lipids and non-saponifiable components of CWO.

There are several research directions from a structure–property perspective that can be pursued to further understand the fundamental mechanisms driving the phase behavior of CWO and improve the thermophysical and bioactivity properties of CWO-based products. These are related to (i) the development of more effective extraction and processing techniques, (ii) the production of novel separation techniques to obtain functional materials with narrower controlled molecular compositions and (iii) the use of modification agents to direct and control phase behavior. The properties of importance to consider include the viscosity and flow properties, and hydrolytic and oxidative stability, which influence the shelf and use life.

**Supplementary Materials:** The following supporting information can be downloaded at: <https://www.mdpi.com/article/10.3390/pr11092565/s1>, Figure S1: ESI-MS spectra of the Crabwood Oil (CWO) and its fractions; Figure S2: TGA and DTG stacks of CWO and its stearin and olein fractions Table S1: Relative abundance percentages of assigned lipids in CWO and its fractions; Table S2: Relative abundance percentages of assigned unsaponifiable components in CWO and its fractions; Table S3: (a) Crystallization and (b) Melting data of CWO and its fractions; Table S4: (a) WAXD and (b) SAXD data.  $\chi$  (%): crystallinity; and Table S5: DTG and TGA data for CWO and its fractions.

**Author Contributions:** Conceptualization, S.O.J., L.B. and S.S.N.; Investigation, S.O.J.; Writing—original draft, S.O.J.; Writing—review & editing, L.B., R.J.N.E. and S.S.N.; Supervision, Laziz Bouzidi, R.J.N.E. and S.S.N. All authors have read and agreed to the published version of the manuscript.

**Funding:** The Sustainable Guyana Program, a partnership between Trent University and the University of Guyana funded by CGX Energy Inc. and Frontera Energy Corporation.

**Data Availability Statement:** All related data is provided in Supporting Information.

**Conflicts of Interest:** The authors declare no conflict of interest.

## References

- Convention on Biological Diversity. Available online: <https://www.cbd.int/countries/profile/?country=gy#:~:text=Forests%20in%20Guyana%20can%20be,most%20part%2C%20intact%20but%20understudied> (accessed on 31 May 2023).
- Firmino, A.V.; Vidaurre, G.B.; Oliveira, J.T.D.S.; Guedes, M.; Almeida, M.N.F.D.; Silva, J.G.M.D.; Latorraca, J.V.D.F.; Zanoncio, J.C. Wood properties of *Carapa guianensis* from floodplain and upland forests in Eastern Amazonia, Brazil. *Sci. Rep.* **2019**, *9*, 10641. [[CrossRef](#)] [[PubMed](#)]
- van Andel, T.; Reinders, M. Non-Timber Forest Products of the North-West District of Guyana. Part 1. 2000. Available online: <https://www.tropenbos.org/resources/publications/non-timber+forest+products+of+the+north-west+district+of+guyana+part+i> (accessed on 31 May 2023).
- Plowden, C. The Ecology and Harvest of Andiroba Seeds for Oil Production in the Brazilian Amazon. *Conserv. Soc.* **2004**, *2*, 251–272.
- Silva, B.A.; Scussel, V.M. Characteristics and Effects of the Amazonian Andiroba (*Carapa guianensis* Aubl.) Oil Against Living Organisms—A Review. *IOSR J. Biotechnol. Biochem. (IOSR-JBB)* **2020**, *6*, 31–47.
- Taylor, L. Technical Data Report for Andiroba. *Herb. Secrets Rainfor.* **2002**, 1–27. Available online: <https://rain-tree.com/reports/andiroba-tech.pdf> (accessed on 31 May 2023).
- Forget, P.-M.; Poncy, O.; Thomas, R.; Hammond, D.; Kenfack, D. A new species of *Carapa* (Meliaceae) from Central Guyana. *Brittonia* **2009**, *61*, 366–374. [[CrossRef](#)]
- Bruna, A.; Neyeli, C.; Cristina, L.; De, C.M.; Vildes, M. Effect of Andiroba (*Carapa guianensis* Aubl.) Oil for Fungi Control in Maize (*Zea mays* L.) Grains. *J. Agric. Vet. Sci.* **2019**, *12*, 26–32.
- Pereira, T.B.; Rocha E Silva, L.F.; Amorim, R.C.; Melo, M.R.; Zacardi De Souza, R.C.; Eberlin, M.N.; Lima, E.S.; Vasconcellos, M.C.; Pohlit, A.M. In vitro and in vivo anti-malarial activity of limonoids isolated from the residual seed biomass from *Carapa guianensis* (andiroba) oil production. *Malar. J.* **2014**, *13*, 4–11. [[CrossRef](#)]
- Nayak, B.S.; Kanhai, J.; Milne, D.M.; Pereira, L.P.; Swanston, W.H. Experimental evaluation of ethanolic extract of *Carapa guianensis* L. leaf for its wound healing activity using three wound models. *Evid.-Based Complement. Altern. Med.* **2011**, *2011*, 419612. [[CrossRef](#)]
- Klauck, V.; Pazinato, L.; Stefani, L.M.; Santos, R.C.; Vaucher, R.A.; Baldiserra, M.D.; Raffin, R.; Boligon, A.; Athayde, M.; Baretta, D.; et al. Insecticidal and repellent effects of tea tree and andiroba oils on flies associated with livestock. *Med. Vet. Entomol.* **2014**, *28*, 33–39. [[CrossRef](#)]
- Araujo-Lima, C.F.; Fernandes, A.S.; Gomes, E.M.; Oliveira, L.L.; Macedo, A.F.; Antoniassi, R.; Wilhelm, A.E.; Aiub, C.A.F.; Felzenszwalb, I. Antioxidant activity and genotoxic assessment of crabwood (andiroba, *Carapa guianensis* Aublet) seed oils. *Oxidative Med. Cell. Longev.* **2018**, *2018*, 3246719. [[CrossRef](#)]
- Dantas, A.R.; Lira-Guedes, A.C.; Mustin, K.; Aparicio, W.C.S.; Guedes, M.C. Phenology of the multi-use tree species *Carapa guianensis* in a floodplain forest of the Amazon Estuary. *Acta Bot. Bras.* **2016**, *30*, 618–627. [[CrossRef](#)]
- Burlando, B.; Cornara, L. Revisiting amazonian plants for skin care and disease. *Cosmetics* **2017**, *4*, 25. [[CrossRef](#)]
- Balbani, A.P.S.; Silva, D.H.S.; Montovani, J.C. Patents of drugs extracted from Brazilian medicinal plants. *Expert Opin. Ther. Pat.* **2009**, *19*, 461–473. [[CrossRef](#)]
- Kennedy, L. Skin Conditioning Compositions Comprising Plant Products. WO2013155527, 7 October 2013.
- IAST Natural Soaps—The Rupununi Essence Project. Available online: [https://iast.gov.gy/?page\\_id=872](https://iast.gov.gy/?page_id=872) (accessed on 29 May 2023).
- Lüdtke, F.L.; Grimaldi, L.M.; Silva, T.J.; Ramponi, K.; de Godoi, R.; Silva, M.G.; Grimaldi, R.; Ribeiro, A.P.B. Physicochemical properties of Andiroba (*Carapa guianensis*) and Pracaxi (*Pentaclethra macroloba*) oils. *Inform* **2021**, *2021*, 30–33. [[CrossRef](#)]

19. Oliveira, I.D.S.D.S.; Moragas Tellis, C.J.; Chagas, M.D.S.D.S.; Behrens, M.D.; Calabrese, K.D.S.; Abreu-Silva, A.L.; Almeida-Souza, F. *Carapa guianensis* Aublet (Andiroba) Seed Oil: Chemical Composition and Antileishmanial Activity of Limonoid-Rich Fractions. *BioMed Res. Int.* **2018**, *2018*, 5032816. [[CrossRef](#)] [[PubMed](#)]
20. Nascimento, G.O.; Souza, D.P.; Santos, A.S.; Batista, J.F.; Rathinasabapathi, B.; Gagliardi, P.R.; Goncalves, J.F.C. Lipidomic profiles from seed oil of *Carapa guianensis* Aubl. and *Carapa vasquezii* Kenfack and implications for the control of phytopathogenic fungi. *Ind. Crops Prod.* **2019**, *129*, 67–73. [[CrossRef](#)]
21. Bataglioni, G.A.; da Silva, F.M.A.; Santos, J.M.; dos Santos, F.N.; Barcia, M.T.; de Lourenço, C.C.; Salvador, M.J.; Godoy, H.T.; Eberlin, M.N.; Koolen, H.H.F. Comprehensive characterization of lipids from Amazonian vegetable oils by mass spectrometry techniques. *Food Res. Int.* **2014**, *64*, 472–481. [[CrossRef](#)]
22. De Sousa, R.L.; Silva, S.G.; Costa, J.M.; Da Costa, W.A.; Maia, A.A.B.; De Oliveira, M.S.; Andrade, E.H.D.A. Chemical profile of manually extracted andiroba oil (*Carapa guianensis* Aubl. Meliaceae) from Mamangal community, located in Igarapé-Miri, Pará, Brazil. *Sci. Plena* **2022**, *17*. [[CrossRef](#)]
23. Dias, K.K.B.; Cardoso, A.L.; da Costa, A.A.F.; Passos, M.F.; da Costa, C.E.F.; da Rocha Filho, G.N.; de Aguiar Andrade, E.H.; Luque, R.; do Nascimento, L.A.S.; Noronha, R.C.R. Biological activities from andiroba (*Carapa guianensis* Aublet.) and its biotechnological applications: A systematic review. *Arab. J. Chem.* **2023**, *16*, 104629.
24. Ferreira, A.M.; da S Sena, I.; Magalhaes, K.F.; Oliveira, S.L.; Ferreira, I.M.; Porto, A.L.M. Amazon Oils from Andiroba (*Carapa* sp.) and Babassu (*Orbignya* sp.) for Preparation Biodiesel by Enzymatic Catalysis. *Curr. Biotechnol.* **2018**, *7*, 428–437. [[CrossRef](#)]
25. Rodrigues de Oliveira, F.; Eleuterio Rodrigues, K.; Hamoy, M.; Rodrigues Sarquis, Í.; Otake Hamoy, A.; Elena Crespo Lopez, M.; Maciel Ferreira, I.; de Matos Macchi, B.; Luiz Martins do Nascimento, J. Fatty Acid Amides Synthesized from Andiroba Oil (*Carapa guianensis* Aublet.) Exhibit Anticonvulsant Action with Modulation on GABA-A Receptor in Mice: A Putative Therapeutic Option. *Pharmaceuticals* **2020**, *13*, 43. [[CrossRef](#)] [[PubMed](#)]
26. Marinho, V.H.S.; Holanda, F.H.; Araújo, I.F.; Jimenez, D.E.Q.; Pereira, R.R.; Porto, A.L.M.; Ferreira, A.M.; Carvalho, J.C.T.; Albuquerque de Freitas, A.C.G.; Fernandes, C.P.; et al. Nanoparticles from silk fibroin and Amazon oils: Potential larvicidal activity and oviposition deterrence against *Aedes aegypti*. *Ind. Crops Prod.* **2023**, *203*, 117133. [[CrossRef](#)]
27. Cusioli, L.F.; Mantovani, D.; Bergamasco, R.; Tusset, A.M.; Lenzi, G.G. Preparation of a New Adsorbent Material from Agro-Industrial Waste and Comparison with Commercial Adsorbent for Emerging Contaminant Removal. *Processes* **2023**, *11*, 2478. [[CrossRef](#)]
28. Serafin, J.; Ouzzine, M.; Cruz, O.F., Jr.; Srenscek-Nazzal, J.; Campello Gomez, I.; Azar, F.-Z.; Rey Mafull, C.A.; Hotza, D.; Rambo, C.R. Conversion of fruit waste-derived biomass to highly microporous activated carbon for enhanced CO<sub>2</sub> capture. *Waste Manag.* **2021**, *136*, 273–282. [[CrossRef](#)] [[PubMed](#)]
29. Lira, G.B.; Lopes, A.; Nascimento, F.; Conceição, G.; Brasil, D. Extraction processes and industrial uses of andiroba and açaí oils: A review. *Res. Soc. Dev.* **2021**, *10*, e229101220227. [[CrossRef](#)]
30. Sarquis, I.R.; Sarquis, R.S.F.R.; Marinho, V.H.S.; Neves, F.B.; Araujo, I.F.; Damasceno, L.F.; Ferreira, R.M.A.; Souto, R.N.P.; Carvalho, J.C.T.; Ferreira, I.M. *Carapa guianensis* Aubl. (Meliaceae) oil associated with silk fibroin, as alternative to traditional surfactants, and active against larvae of the vector *Aedes aegypti*. *Ind. Crops Prod.* **2020**, *157*, 112931. [[CrossRef](#)]
31. Iha, O.K.; Alves, F.C.; Suarez, P.A.; Silva, C.R.; Meneghetti, M.R.; Meneghetti, S.M. Potential application of *Terminalia catappa* L. and *Carapa guianensis* oils for biofuel production: Physical-chemical properties of neat vegetable oils, their methyl-esters and bio-oils (hydrocarbons). *Ind. Crops Prod.* **2014**, *52*, 95–98. [[CrossRef](#)]
32. Tong, S.-C.; Tang, T.-K.; Lee, Y.-Y. A Review on the Fundamentals of Palm Oil Fractionation: Processing Conditions and Seeding Agents. *Eur. J. Lipid Sci. Technol.* **2021**, *123*, 2100132. [[CrossRef](#)]
33. Zhang, Z.; Ma, X.; Huang, H.; Wang, Y. Shea olein based specialty fats: Preparation, characterization and potential application. *LWT* **2017**, *86*, 492–500. [[CrossRef](#)]
34. Perederic, O.A.; Mansouri, S.S.; Appel, S.; Sarup, B.; Gani, R.; Woodley, J.M.; Kontogeorgis, G.M. Process Analysis of Shea Butter Solvent Fractionation Using a Generic Systematic Approach. *Ind. Eng. Chem. Res.* **2020**, *59*, 9152–9164. [[CrossRef](#)]
35. Minzangi, K.; Kadima, J.N.; Kaaya, A.N.; Matthäus, B.; Van Damme, P.; Samvura, B.; Mosibono, D.E.; Belesi, K.; Mpiana, P.T. Fatty acids and tocopherols content in fractionated oils from five wild oilseed plants Native to Kahuzi-Biega National Park, Kivu-DR Congo. *Eur. J. Med. Plants* **2015**, *10*, 1–9. [[CrossRef](#)]
36. Kazadi, M.; Bokota, M.T.; Mpiana, P.T. Potential New Sources of Oleic Acids from Wild Plants from Kivu, D. R. Congo. *J. Phys. Chem. Sci.* **2014**, *1*, 1–4.
37. National Center for Biotechnology Information. PubChem Compound Summary for CID 8857, Ethyl Acetate. Available online: <https://pubchem.ncbi.nlm.nih.gov/compound/8857> (accessed on 18 August 2023).
38. Health, C.P. (Ed.) Reference Manual—Consumer Chemicals and Containers Regulations, 2001. 2007. Available online: [https://www.canada.ca/content/dam/hc-sc/migration/hc-sc/cps-spc/alt\\_formats/hecs-sesc/pdf/pubs/indust/cccr-2001-rpccc/ref\\_man/cccr-rpccc3-eng.pdf](https://www.canada.ca/content/dam/hc-sc/migration/hc-sc/cps-spc/alt_formats/hecs-sesc/pdf/pubs/indust/cccr-2001-rpccc/ref_man/cccr-rpccc3-eng.pdf) (accessed on 18 August 2023).
39. National Center for Biotechnology Information. PubChem Compound Summary for CID 180, Acetone. Available online: <https://pubchem.ncbi.nlm.nih.gov/compound/180> (accessed on 18 August 2023).
40. National Center for Biotechnology Information. PubChem Compound Summary for CID 702, Ethanol. Available online: <https://pubchem.ncbi.nlm.nih.gov/compound/Ethanol> (accessed on 18 August 2023).

41. Cheng, X.; Hochlowski, J. Current application of mass spectrometry to combinatorial chemistry. *Anal. Chem.* **2002**, *74*, 2679–2690. [[CrossRef](#)]
42. Milward, S. Greasing the Wheels for Conservation and Development: Can Crabwood Oil Enterprises Contribute to Sustainable Development of the Riverine Communities in North Rupununi, Central Guyana? A Study of Enterprise Development. Ph.D. Thesis, University of Leeds, Leeds, UK, 2002. (Unpublished work).
43. Pillai, P.K.S.; Li, S.; Bouzidi, L.; Narine, S.S. Metathesized palm oil: Fractionation strategies for improving functional properties of lipid-based polyols and derived polyurethane foams. *Ind. Crops Prod.* **2016**, *84*, 273–283. [[CrossRef](#)]
44. Abubakar, A.R.; Haque, M. Preparation of Medicinal Plants: Basic Extraction and Fractionation Procedures for Experimental Purposes. *J. Pharm. Bioallied Sci.* **2020**, *12*, 1–10. [[CrossRef](#)] [[PubMed](#)]
45. Ghotra, B.S.; Dyal, S.D.; Narine, S.S. Lipid shortenings: A review. *Food Res. Int.* **2002**, *35*, 1015–1048. [[CrossRef](#)]
46. Marangoni, A.G.; Wesdorp, L.H. *Structure and Properties of Fat Crystal Networks*, Second Edition, 2nd ed.; Taylor & Francis: New York, NY, USA, 2012.
47. Raghunanan, L.; Floros, M.C.; Narine, S.S. Thermal stability of renewable diesters as phase change materials. *Thermochim. Acta* **2016**, *644*, 61–68. [[CrossRef](#)]
48. National Center for Biotechnology Information. PubChem. Available online: <https://pubchem.ncbi.nlm.nih.gov/> (accessed on 20 February 2023).
49. Goncalves Bonassoli, A.B.; Oliveira, G.; Bordon Sosa, F.H.; Rolemberg, M.P.; Mota, M.A.; Basso, R.C.A.; Igarashi-Mafra, L.; Mafra, M.R. Solubility measurement of lauric, palmitic, and stearic acids in ethanol, n-propanol, and 2-propanol using differential scanning calorimetry. *J. Chem. Eng. Data* **2019**, *64*, 2084–2092. [[CrossRef](#)]
50. MetaboQuest, omicraft: Washington, DC, USA, 2023. Available online: <http://tools.omiccraft.com/MetaboQuest/> (accessed on 20 February 2023).
51. LIPIDMAPS. Available online: <https://lipidmaps.org/> (accessed on 20 February 2023).
52. Saraiva, S.A.; Cabral, E.C.; Eberlin, M.N.; Catharino, R.R. Amazonian vegetable oils and fats: Fast typification and quality control via triacylglycerol (TAG) profiles from dry matrix-assisted laser desorption/ionization time-of-flight (MALDI-TOF) mass spectrometry fingerprinting. *J. Agric. Food Chem.* **2009**, *57*, 4030–4034. [[CrossRef](#)]
53. Cabral, E.C.; da Cruz, G.F.; Simas, R.C.; Sanvido, G.B.; Goncalves, L.D.V.; Leal, R.V.P.; da Silva, R.C.F.; da Silva, J.C.T.; Barata, L.E.S.; da Cunha, V.S.; et al. Typification and quality control of the Andiroba (*Carapa guianensis*) oil via mass spectrometry fingerprinting. *Anal. Methods* **2013**, *5*, 1385–1391. [[CrossRef](#)]
54. Gibon, V.; De Greyt, W.; Kellens, M. Palm oil refining. *Eur. J. Lipid Sci. Technol.* **2007**, *109*, 315–335. [[CrossRef](#)]
55. Nakamura, M.T.; Yudell, B.E.; Loor, J.J. Regulation of energy metabolism by long-chain fatty acids. *Prog. Lipid Res.* **2014**, *53*, 124–144. [[CrossRef](#)] [[PubMed](#)]
56. Kametani, S.; Kojima-Yuasa, A.; Kikuzaki, H.; Kennedy, D.O.; Honzawa, M.; Matsui-Yuasa, I. Chemical Constituents of Cape Aloe and Their Synergistic Growth-Inhibiting Effect on Ehrlich Ascites Tumor Cells. *Biosci. Biotechnol. Biochem.* **2007**, *71*, 1220–1229. [[CrossRef](#)]
57. PubChem, Compound Summary for CID 5312773, 18-Hydroxyoleic acid. National Center for Biotechnology Information. 2023. Available online: <https://pubchem.ncbi.nlm.nih.gov/compound/18-Hydroxyoleic-acid> (accessed on 31 May 2023).
58. Kishino, S.; Takeuchi, M.; Park, S.-B.; Hirata, A.; Kitamura, N.; Kunisawa, J.; Kiyono, H.; Iwamoto, R.; Isobe, Y.; Arita, M. Polyunsaturated fatty acid saturation by gut lactic acid bacteria affecting host lipid composition. *Proc. Natl. Acad. Sci. USA* **2013**, *110*, 17808–17813. [[CrossRef](#)] [[PubMed](#)]
59. Whelan, J.; Fritsche, K. Linoleic acid. *Adv. Nutr.* **2013**, *4*, 311–312. [[CrossRef](#)]
60. Adarme-Vega, T.C.; Thomas-Hall, S.R.; Schenk, P.M. Towards sustainable sources for omega-3 fatty acids production. *Curr. Opin. Biotechnol.* **2014**, *26*, 14–18. [[CrossRef](#)]
61. Stoveken, H.M.; Larsen, S.D.; Smrcka, A.V.; Tall, G.G. Gedunin- and Khivorin-Derivatives Are Small-Molecule Partial Agonists for Adhesion G Protein-Coupled Receptors GPR56/ADGRG1 and GPR114/ADGRG5. *Mol. Pharmacol.* **2018**, *93*, 477–488. [[CrossRef](#)]
62. Abdelgaleil, S.A.; Hashinaga, F.; Nakatani, M. Antifungal activity of limonoids from *Khaya ivorensis*. *Pest Manag. Sci.* **2005**, *61*, 186–190. [[CrossRef](#)] [[PubMed](#)]
63. Chiruvella, K.K.; Kari, V.; Choudhary, B.; Nambiar, M.; Ghanta, R.G.; Raghavan, S.C. Methyl angolensate, a natural tetranortriterpenoid induces intrinsic apoptotic pathway in leukemic cells. *FEBS Lett.* **2008**, *582*, 4066–4076. [[CrossRef](#)]
64. Chiruvella, K.K.; Panjamurthy, K.; Choudhary, B.; Joy, O.; Raghavan, S.C. Methyl angolensate from callus of Indian redwood induces cytotoxicity in human breast cancer cells. *Int. J. Biomed. Sci. IJBS* **2010**, *6*, 182–194.
65. Chiruvella, K.K.; Mohammed, A.; Dampuri, G.; Ghanta, R.G.; Raghavan, S.C. Phytochemical and Antimicrobial Studies of Methyl Angolensate and Luteolin-7-O-glucoside Isolated from Callus Cultures of *Soymida febrifuga*. *Int. J. Biomed. Sci. IJBS* **2007**, *3*, 269–278.
66. Nakatani, M.; James, J.C.; Nakanishi, K. Isolation and structures of trichilins, antifeedants against the Southern army worm. *J. Am. Chem. Soc.* **1981**, *103*, 1228–1230. [[CrossRef](#)]
67. Vieira, I.; Terra, W.; Gonçalves, M.; Braz-Filho, R. Secondary Metabolites of the Genus *Trichilia*: Contribution to the Chemistry of Meliaceae Family. *Am. J. Anal. Chem.* **2014**, *5*, 91–121. [[CrossRef](#)]
68. Fokam, M.A.M.; Mfifen, A.M.; Nkengfack, A.E. Isolation, characterization and cytotoxic activity of isolated compounds from seed of *Carapa angustifolia* (Meliaceae). *J. Chem. Pharm. Res.* **2019**, *11*, 7–10.

69. Gonzalez-Ramirez, M.; Limachi, I.; Manner, S.; Ticona, J.C.; Salamanca, E.; Gimenez, A.; Sterner, O. Trichilones A–E: New Limonoids from *Trichilia adolfi*. *Molecules* **2021**, *26*, 3070. [[CrossRef](#)] [[PubMed](#)]
70. Braga, T.M.; Rocha, L.; Chung, T.Y.; Oliveira, R.F.; Pinho, C.; Oliveira, A.I.; Morgado, J.; Cruz, A. Biological Activities of Gedunin-A Limonoid from the Meliaceae Family. *Molecules* **2020**, *25*, 493. [[CrossRef](#)]
71. Sakamoto, A.; Tanaka, Y.; Inoue, T.; Kikuchi, T.; Kajimoto, T.; Muraoka, O.; Yamada, T.; Tanaka, R. Andriolides Q–V from the flower of andiroba (*Carapa guianensis*, Meliaceae). *Fitoterapia* **2013**, *90*, 20–29. [[CrossRef](#)] [[PubMed](#)]
72. Bortolozzi, R.; Luraghi, A.; Mattiuzzo, E.; Sacchetti, A.; Silvani, A.; Viola, G. Ecdysteroid Derivatives that Reverse P-Glycoprotein-Mediated Drug Resistance. *J. Nat. Prod.* **2020**, *83*, 2434–2446. [[CrossRef](#)] [[PubMed](#)]
73. Metin, S.; Hartel, R.W. Fundamentals of Lipid Crystallization. In *Bailey's Industrial Oil and Fat Products*; Wiley: Hoboken, NJ, USA, 2020; pp. 1–31. [[CrossRef](#)]
74. Minato, A.; Ueno, S.; Smith, K.; Amemiya, Y.; Sato, K. Thermodynamic and kinetic study on phase behavior of binary mixtures of POP and PPO forming molecular compound systems. *J. Phys. Chem. B* **1997**, *101*, 3498–3505. [[CrossRef](#)]
75. Bayes-Garcia, L.; Calvet, T.; Cuevas-Diarte, M.À.; Ueno, S.; Sato, K. Phase behavior of binary mixture systems of saturated-unsaturated mixed-acid triacylglycerols: Effects of glycerol structures and chain–chain interactions. *J. Phys. Chem. B* **2015**, *119*, 4417–4427. [[CrossRef](#)] [[PubMed](#)]
76. Gibon, V.; Danthine, S. Systematic Investigation of Co-Crystallization Properties in Binary and Ternary Mixtures of Triacylglycerols Containing Palmitic and Oleic Acids in Relation with Palm Oil Dry Fractionation. *Foods* **2020**, *9*, 1891. [[CrossRef](#)]
77. Patel, S.; Nelson, D.R.; Gibbs, A.G. Chemical and physical analyses of wax ester properties. *J. Insect Sci.* **2001**, *1*, 4. [[CrossRef](#)] [[PubMed](#)]
78. Mullin, J.W. *Crystallization*, 4th ed.; Butterworth-Heinemann: Oxford, UK, 2001; p. 600.
79. Bouzidi, L.; Narine, S.S. Evidence of Critical Cooling Rates in the Nonisothermal Crystallization of Triacylglycerols: A Case for the Existence and Selection of Growth Modes of a Lipid Crystal Network. *Langmuir* **2010**, *26*, 4311–4319. [[CrossRef](#)]
80. Rousseau, D.; Marangoni, A.G.; Jeffrey, K.R. The influence of chemical interesterification on the physicochemical properties of complex fat systems. 2. Morphology and polymorphism. *J. Am. Oil Chem. Soc.* **1998**, *75*, 1833–1839. [[CrossRef](#)]
81. Narine, S.S.; Marangoni, A.G. Fractal nature of fat crystal networks. *Phys. Rev. E* **1999**, *59*, 1908–1920. [[CrossRef](#)]
82. Marangoni, A.G.; Narine, S.S. Identifying key structural indicators of mechanical strength in networks of fat crystals. *Food Res. Int.* **2002**, *35*, 957–969. [[CrossRef](#)]
83. Gosselink, R.W.; Hollak, S.A.W.; Chang, S.-W.; van Haveren, J.; de Jong, K.P.; Bitter, J.H.; van Es, D.S. Reaction Pathways for the Deoxygenation of Vegetable Oils and Related Model Compounds. *ChemSusChem* **2013**, *6*, 1576–1594. [[CrossRef](#)] [[PubMed](#)]
84. Vonghia, E.; Boocock, D.G.; Konar, S.K.; Leung, A. Pathways for the deoxygenation of triglycerides to aliphatic hydrocarbons over activated alumina. *Energy Fuels* **1995**, *9*, 1090–1096. [[CrossRef](#)]
85. Wilson, B. Lubricants and functional fluids from renewable sources. *Ind. Lubr. Tribol.* **1998**, *50*, 6–15. [[CrossRef](#)]
86. Niu, S.; Zhou, Y.; Yu, H.; Lu, C.; Han, K. Investigation on thermal degradation properties of oleic acid and its methyl and ethyl esters through TG-FTIR. *Energy Convers. Manag.* **2017**, *149*, 495–504. [[CrossRef](#)]
87. Alves, C.T.; Peters, M.A.; Onwudili, J.A. Application of thermogravimetric analysis method for the characterisation of products from triglycerides during biodiesel production. *J. Anal. Appl. Pyrolysis* **2022**, *168*, 105766.
88. Vecchio, S.; Campanella, L.; Nuccilli, A.; Tomassetti, M. Kinetic study of thermal breakdown of triglycerides contained in extra-virgin olive oil. *J. Therm. Anal. Calorim.* **2008**, *91*, 51–55. [[CrossRef](#)]

**Disclaimer/Publisher's Note:** The statements, opinions and data contained in all publications are solely those of the individual author(s) and contributor(s) and not of MDPI and/or the editor(s). MDPI and/or the editor(s) disclaim responsibility for any injury to people or property resulting from any ideas, methods, instructions or products referred to in the content.